Geophys. J. R. astr. Soc. (1986) **84**, 529–559

A seismic refraction survey in the Kerguelen Isles, southern Indian Ocean

Maurice Recq *Département de Géologie Dynamique, Groupe d'Etude de la Marge Continentale (UA 718 du CNRS), Université Pierre et Marie Curie, 4 Place Jussieu, 75230 Paris Cedex 05, France*

Philippe Charvis* *Département de Géologie Dynamique, Groupe d'Etude de la Marge Continentale (UA 718 du CNRS), Université Pierre et Marie Curie, 4 Place Jussieu, 75230 Paris Cedex 05, France and Institut de Physique du Globe de Paris, Laboratoire d'Etude Géophysique des Structures Profondes (LA 195 du CNRS), Université Pierre et Marie Curie, 4 Place Jussieu, 75230 Paris Cedex 05, Paris*

Accepted 1985 July 25. Received 1985 July 18; in original form 1984 December 27

Summary. Two 65 km long on-land refraction lines, with shot detonated at sea, were implemented in the Courbet Peninsula, eastern region of the Kerguelen archipelago (Terres Australes et Antarctiques Françaises, southern Indian Ocean). The first profile P1, oriented NE–SW, runs from Cap Ratmanoff toward Mont Ross, and the second one, P2, from Pointe Suzanne, SE of the Courbet Peninsula, through the Val Studer. Data from both profiles were supplemented by using the Bouguer gravity anomaly map not previously studied. The data combined standard travel-time interpretation, wide-angle reflected wave study, synthetic seismograms and *S*-wave analysis. The velocity–depth behaviour shows that the mean crustal thickness ranges from 14 to 17 km only, varying with the locality. The structure of the crust beneath Kerguelen resembles those observed beneath aseismic ridges (i.e. the Crozet Rise and the Madagascar Ridge). Average velocity of 5.5 km s^{-1} on both lines is in the range of those determined for oceanic layer 2, which is there 8–9 km thick. Average velocity of 6.6 km s^{-1} is in the range of velocities within oceanic layer 3. The transition to mantle velocity, 7.95 km s^{-1} is best modelled by a positive velocity gradient within the crust. This feature is similar to that observed on structures generated near spreading centres. These new data combined with geological and geochemical investigations in the archipelago support an oceanic origin for the Kerguelen–Heard Ridge, and also Broken Ridge. Both structures were joined 40 Myr ago, as shown by the magnetic anomaly pattern. Refraction studies invalidate the assumption that isostatic compensation is achieved by a 23 km deep crustal root, but substantiate the

* Now at Office de la Recherche Scientifique et Technique d'Outre-Mer (ORSTOM), BP A5 Nouméa Cedex, New Caledonia.

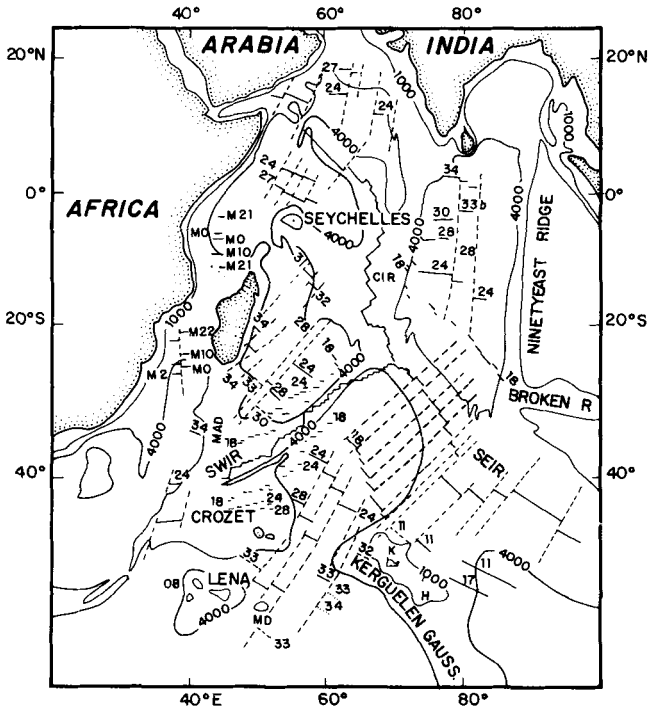

Figure 1. Bathymetry depth contours in metres, major physiography, magnetic anomaly identifications and fracture zones of the SW Indian Ocean after Schlich (1983), Goslin & Patriat (1984). CIR: Central Indian Ridge; SEIR: SE Indian Ridge; SWIR: SW Indian Ridge. MD and OB: Marion Dufresne and Ob seamounts; K: Kerguelen; H: Heard Islands.

contribution of a low velocity mantle. Gravity data are consistent with refraction studies. No crustal root appears to be present beneath Mont Ross. The best match between gravity and refraction data in the Val Studer is obtained by assuming the presence of a shallow intrusive body, related to the fault and dyke system, and Montagnes Vertes plutonic intrusive complex nearby.

Key words: aseismic ridge, Kerguelen, oceanic

Introduction

The Kerguelen Archipelago and Heard Island, located 500 km southward, are subaerial parts of the Kerguelen–Heard aseismic Ridge, known also as the Kerguelen–Gaussberg Ridge (Fig. 1). It extends from 46 to 64°S, in a NNW–SSE direction with an average width of 450 km. The Kerguelen–Gaussberg Ridge is bounded north and east by the oceanic Crozet Basin, SW by the Enderby Basin, and SE by the Australia–Antarctic Basin (Fig. 1); the latter separates the Kerguelen–Heard Ridge from Broken Ridge and the Naturaliste Plateau. A trough, down to 3600 m deep, named the Challenger Channel (Vanney & Johnson 1982), separates the Kerguelen–Heard Ridge from the Antarctic margins.

The large region (1000 m below sea-level), extending from 46 to 55°S, where the islands of Kerguelen and Heard are located, forms the northern part of the ridge which is affected by steep faulting and covered by sediment layers up to 2500 m thick, whereas the part of the ridge, running from 58 to 64°S lies at greater depth and exhibits a more subdued topography, with a more uniform sedimentation (Houtz, Hayes & Markl 1977; Schlich

1983). Both flanks of the Kerguelen–Gaussberg Ridge appear to be more rugged south of 54°S.

A rather confused topography with a westward stretched spur over a range of 600 km are the main features of the transition zone between 55 and 58°S (Houtz *et al.* 1977; Goslin & Patriat 1984). Extremely high amplitude and short wavelength magnetic anomalies denote a shallow basaltic basement of the ridge (Schlich 1975; Goslin 1981).

Between Broken Ridge and the Kerguelen–Heard Ridge, Le Pichon & Heirtzler (1968), and Houtz *et al.* (1977) identified magnetic anomalies 17 and 18 of late Eocene time, alongside the north-eastern flank of the northern part of the Kerguelen–Gaussberg Ridge.

In the past decades, using data from the oceanic cruises of *M/V Galliéni* and from 1973, of *N/O Marion Dufresne,* both operated by the Administration des Terres Australes et Antarctiques Françaises (TAAF), Schlich (1975) observed the entire sequence of Cretaceous magnetic anomalies, NE of the Kerguelen–Heard Ridge. In the Australia–Antarctic Basin, in the neighbourhood of Heard Island, magnetic anomaly 11 has been previously identified by Schlich & Patriat (1971). Southernmost, anomalies 17 and 18 (upper Eocene) were recognized on the basaltic basement (McKenzie & Sclater 1971; Schlich 1975; Houtz *et al.* 1977). NE of Kerguelen Islands, Goslin (1981) identified anomalies 12, 13, 15 and maybe 18. The ridge is probably synchronous with the nearby deep ocean basin (Goslin & Patriat 1984).

Broken Ridge and the Kerguelen–Gaussberg Ridge lie symmetrically with respect to the general direction of the SE Indian Ridge. Le Pichon & Heirtzler (1968), previously noticed the symmetry of the magnetic anomaly pattern on either side of this spreading ridge. This pattern suggests that: (a) Australia has been separated from Antarctica at Middle Eocene time; (b) Broken Ridge must at one time have been joined to Kerguelen, 40 Myr ago (McKenzie & Sclater 1971); although limited overlaps of two plateaus are shown by reconstruction, it appears that Mutter & Cande (1983) have reconciled this figure.

The subaerial surface of the Kerguelen Isles has an area of 9000 km^2. The main island is 150 km wide and consists principally of Hawaiian-type flood basalts (85 per cent of the surface), with stratovolcanoes (Mont Ross, 1850 m and Société Géographique, 1000 m, being the most important features). The numerous plutonic complexes are of several different types. The largest one lies (Fig. 2) in the Rallier du Baty Peninsula (Nougier 1970). A very important glacier, named Glacier Cook, is located in the centre of the main island. According to Rouillon (private communication), the ice thickness is up to 400 m. The morphology of the Kerguelen Isles is affected by intense glacial erosion as depicted by moraines and numerous fjords (Roth 1875; Studer 1889; Von Drygalski 1912; Aubert de la Rüe 1932; Nougier 1970; Watkins *et al.* 1974).

According to Nougier (1970), the Kerguelen–Heard Ridge had been created during the Eocene. The oldest flood basalts are aged 27 Myr, Oligocene time (Dosso *et al.* 1979; Lameyre *et al.* 1981). Frequent flood eruptions occurred until the Pliocene, superimposed by more recent (Quaternary) stratovolcanoes (Nougier 1970, 1972). An important fumarollic field has been discovered in the Rallier du Baty Peninsula and some fumaroles on Saint-Paul Isles (Bauer & Berthois 1963; Nougier, Ballestracci & Blavoux 1982). Plutonic rocks appear as granitoid intrusive ring complexes (gabbros, syenites, alkaline granites) in the Rallier du Baty Peninsula (Fig. 2). These plutonic rocks are spread over 3 per cent (200 km^2) of the subaerial surface of the Kerguelen Isles.

The origin, whether oceanic or continental, of the Kerguelen Isles and the Kerguelen–Gaussberg Ridge has remained a query for a long time and was already being discussed after the voyages of the British *HMS Challenger* in 1878 (Murray & Renard 1885) and the German vessels *Gazelle* (1874–76) (Studer 1889) and *Gauss* (1901–3) (Von Drygalski 1912).

The following question: 'Ist Kerguelen eine ozeanische oder kontinentale Insel?', was

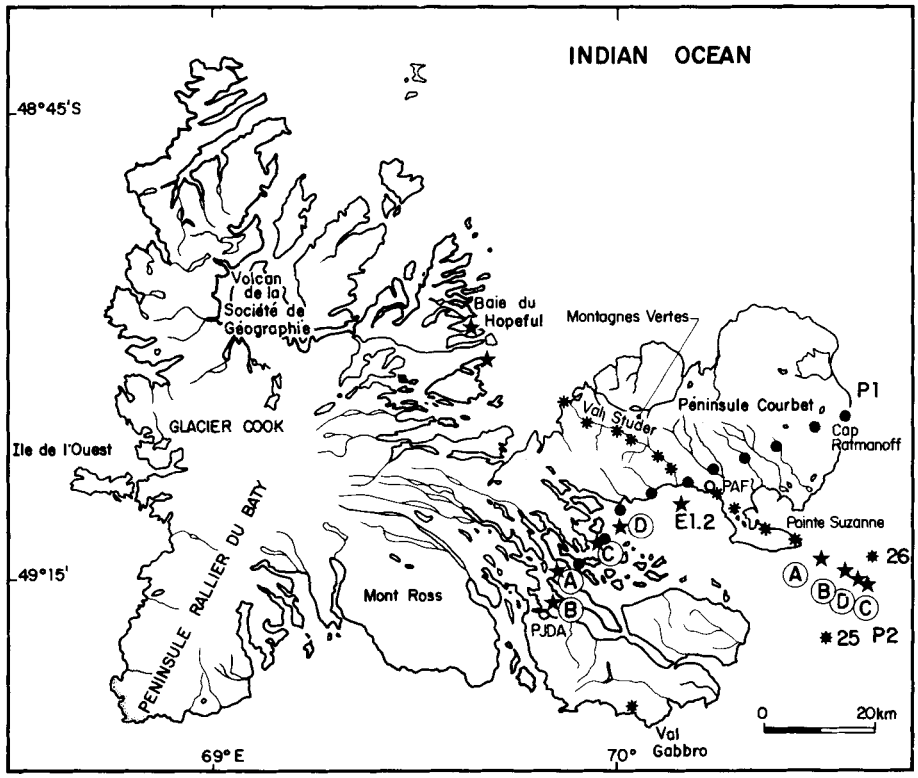

Figure 2. General features of the Kerguelen Isles. The archipelago consists of 400 islands. On-land stations are marked by solid circles on profile P1, running from Cap Ratmanoff towards Mont Ross, and by asterisks on profile P2, running from Pointe Suzanne toward the Baie du Hopeful, through the Val Studer. Stars denote shot points on both profiles. Profiles EL 47–25 and EL 47–26 implemented by Houtz *et al.* (1977) during the *R/V Eltanin* cruise are also plotted (25 and 26). PAF: Port-aux-Français; PJDA: Port-Jeanne d'Arc.

already put by Philippi (1912) 62 years before that from Watkins *et al.* (1974: 'Kerguelen: continental fragment or oceanic island?'. Studer (1878), from geological, fauna and floral studies, emphasized a continental origin, while Chun (1900) believed in an oceanic origin for the Kerguelen Isles that were created and became islands in the Early Tertiary. Philippi (1912) noticed that the Kerguelen and Heard Islands were subaerial domains of an extended submarine plateau running from Kergueien towards Antarctica. This author quoted the existence in Heard Island of hot springs, fumarolles and even calcareous rock 50 years earlier than Stephenson (1964). Roth (1875) was the first geologist to report the presence of carbonate rocks in Kerguelen at the northern end of the main island, near Port Christmas. It appears that the work implemented by these pioneers was under-rated.

More recent investigations show that the Kerguelen Isles and the Kerguelen–Gaussberg Ridge exhibit some features consistent with either a 'sialic microcontinent', or a fragment of a continental crust which could be separated from the Australian margin by the SE Indian Ridge (Heezen & Tharp 1965; Wilson 1965; Dietz & Holden 1970). The scarcity of acid plutonic rocks within oceanic domains, although they are very usual in a continental structure, led Nougier & Lameyre (1973) to consider at once the Kerguelen Isles to be continental.

The first seismic reflection profiles performed over the Kerguelen–Heard Ridge in 1970, during the *Galliéni 3* cruise (Schlich *et al.* 1971) revealed a thick sedimentary layer (2.5 s twt) edged to the south of Kerguelen by a trough of the same scale as the thickness of the sedimentary series and, similarly, towards the north of the archipelago, but with a less striking rise. The general feature, faulted, evoked distensive tectonics over a crystalline basement and so, too hastily, a continental-like sedimentation. Meanwhile, Schlich (1975), Norton & Molnar (1977), from magnetic anomaly surveys, considered a composite solution probable: the northern domain of the Kerguelen–Gaussberg Ridge would be oceanic, whereas the southernmost one might be a fragment of continental crust. Rounded basalt pebbles and the presence of a 1300 m deep truncated outcrop suggest subaerial erosion preceding more recent subsidence (Ewing, Houtz & Hayes 1972). Le Pichon & Heirtzler (1968) and afterwards McKenzie & Sclater (1971) stated that Broken Ridge and the Kerguelen–Gaussberg Ridge were joined before anomaly 17 time. The preliminary refraction lines conducted on Broken Ridge (Francis & Raitt 1967) appeared to support the assumption of a 'quasi-continental' origin for this feature. The hypothesis of a crustal uplift (Zhivago 1965) is inconsistent with the magnetic anomaly pattern and relationships between the Kerguelen–Gaussberg Ridge and Broken Ridge. Wicquart (1983) and Fröhlich *et al.* (1983) reported that the oldest pelagian sediments are 100 Myr old (late Cretaceous). Their deposits just followed the initial stage of the Indian Ocean spreading.

Deep seismic soundings in the Kerguelen archipelago

Until 1983, no refraction data dealing with the deep structure of the crust beneath the Kerguelen Isles and the Kerguelen–Heard Ridge were available. In 1975, an attempt to perform a refraction line on the Ridge, near Kerguelen, during the MD 11 cruise of *N/O Marion Dufresne* failed, caused by too severe weather conditions. The seismic source was Aquaseis, a line explosive up to 100 m in length detonated about 10 m beneath the sea surface. This technique was carried out successfully to investigate the structure of the Crozet Rise and the Madagascar Basin (Goslin, Recq & Schlich 1981a; Recq & Goslin 1981). Short-range refraction lines were conducted using air guns as a seismic source and expendable sonobuoys in the vicinity of the Kerguelen Isles (Fig. 2) and south of Heard Island (Fig. 13) by Houtz *et al.* (1977) during the *R/V Eltanin* cruise. Only information upon the shallow structure of the crust was acquired. The EL47-26 line performed near the archipelago (Fig. 2) in shallow water, 80 m deep, indicated the presence of a 1.7 km thick layer with a mean velocity of 4.15 km s^{-1}, overlaying a basement with a velocity of 5.25 km s^{-1}. This latter velocity is in the range of that observed within the oceanic layer 2. The velocity of 3.10 km s^{-1} on profile EL47-26 fired near EL47-25 (Fig. 2), has been related to material close to the sea bottom.

A preliminary on land seismic refraction survey was carried out in the Kerguelen Isles in 1983 March at the time of the TAAF austral summer campaign. This was a joint programme involving the Groupe d'Etude de la Marge Continentale (Unité Associée au CNRS 718) and the Laboratoire d'Etude Géophysique des Structures Profondes (Laboratoire Associé au CNRS 195) of the Institut de Physique du Globe de Paris (IPGP). Both laboratories are part of the Université Pierre et Marie Curie in Paris. TAAF provided funding and logistical assistance.

In order to appraise the feasibility of this kind of experiment in the Kerguelen Isles, seismic lines were implemented in the vicinity of Port-aux-Français (PAF) base located on the shore of the Courbet Peninsula (Fig. 2). Locations of proposed profiles and shot points (Fig. 2) were defined taking into account geological features with the assistance of Jacques

Nougier. Ranges of seismic lines were up to 65 km long, with seismometers spaced on average 6 km apart. For a few shots, additional records were acquired by the permanent seismological observatory PAF using different recorder settings. The 11 three-component self-triggering mobile stations were supplied by IPGP and redesigned in order to insulate the electronics from humidity prevailing in the Kerguelen Isles. Ten stations were deployed on land using two helicopters Alouette II of the French Armée de l'Air.

Twelve shots, including two test shots, were fired over a less than 90 m deep sea bottom, along a series of lines extending between PAF and Port-Jeanne-d'Arc (PJDA), toward the archipelago centre, and from off Pointe Suzanne through the Val Studer (Fig. 2). Charges consisted of 25, 50 and 100 kg of Géonite. The detonator was crimped on to a slow-burning fuse which was ignited prior to jettisoning explosives (25 and 50 kg charges) off the stern of the 15 m long firing ship *La Japonaise*. Two 100 kg shots were electrically fired north of the Val Studer (Fig. 2). Unusually good weather conditions for the region and for the season (late austral summer), with the exception of a few windy days in the Val Studer, favoured the achievement of very reliable seismic records with a low background noise.

The profile P1 (Fig. 2) running NE–SW from Cap Ratmanoff, east of Kerguelen, to Port-Jeanne d'Arc, towards Mont Ross volcano, traverses the Courbet Peninsula fluvioglacial plain. East of Pointe Molloy, land stations were set up on small islands. One 50 kg charge was fired off PAF, one 50 kg and three 25 kg charges were fired between PAF and PJDA. On the P2 line, oriented NW–SE, extending throughout the Val Studer toward Pointe Suzanne, three 50 kg and one 25 kg charges were fired off Pointe Suzanne and one 50 kg charge off PAF. North of Val Studer, two 100 kg charges, A and B, were fired in the Baie du Hopeful. Some records from these shots are of poor quality caused by a strong wind blowing through the Val Studer. However, both 100 kg charges were surprisingly not as efficient as the other ones, as shown on seismograms from stations off Val Studer: the northernmost one and those spread between PAF and Pointe Suzanne (Fig. 2). Amplitudes are lower than expected by the size of the charges. Two reasons may be put forward, either an incomplete detonation, or the existence of a deep discontinuity across the Baie du Hopeful between the shot points and the on-land refraction line P2.

The flight time of charges ranged from 48 to 60 s, far less than the expected 80 s, thus some charge sizes were reduced to 25 kg. According to White & Bunch (1978) and Duschenes (1983), mean sink rates for 25 and 50 kg charges range from 1.0 to 1.5 m s^{-1}, the charges being detonated near or on the shallow seabottom, as shown by the length of the bubble pulse (Arons, Slifko & Carter 1948; Duschenes 1983).

One of the set of mobile stations was fitted with two geophones bolted to the inside of the small ship's hull in order to determine the instant time of shots. The arrival times of the direct wave were recorded. The distance travelled between the launch of the charge and its detonation was calculated from log readings. An echosounder gave the depth of the seafloor which was always less than 90 m. Regarding the shallow seafloor, we notice that the travel times of the direct wave between a charge detonating at the sea surface and one detonating on the seafloor differ only by less than 0.01 s. Shots A and B were electrically fired from the shore; the electric pulse of the ignition was recorded on the same mobile station set up on land.

The site of the mobile stations was at low altitude, less than 150 m elevation; meanwhile, corrections to travel times were applied with respect to sea-level. Despite the lack of data on seismic velocities within superficial layers, an average velocity of 3.20 km s^{-1} underneath the Plioquaternary layer has been assumed in the calculation of the basement depths from refraction data. This value is close to that for the profile EL47-26 shot in the vicinity of the archipelago over the 80 m deep sea bottom. Velocities of 3.20 km s^{-1} inferred from Houtz

et al.'s (1977) experiments are observed on ridge crests (Talwani, Windisch & Langseth 1971), on volcanic seafloor near Iceland (Johnson & Palmason 1980), and over volcanic islands such as Iceland and Hawaii which are investigated for a long time. In Iceland, velocities ranging from 3.0 to 3.4 km s^{-1} have been ascribed by Palmason (1970) to Quaternary volcanic material predominantly basaltic in composition. In Hawaii, according to Ryall & Bennett (1968), Hill (1969), Zucca & Hill (1980) and Zucca, Hill & Kouach (1982), these velocities represent material from the most recent lavas erupted from volcanoes, both as lava flows. The geological setting of the Courbet Peninsula, as depicted by Nougier (1970) resembles that observed over Iceland.

Corrections to travel times can be expressed by the following formula:

$$\delta t \text{ (in s)} = \delta h_1 (V_i^2 - V_1^2)^{1/2} / V_1' V_i - \delta h_2 (V_i^2 - V_1^2)^{1/2} / V_1 V_i,$$

where:

δh_1: depth (in km) of the seafloor where the charges were detonated;

δh_2: elevation (in km) of the mobile stations;

$V_1' = 1.5$ km s^{-1}, assumed velocity in sea water;

$V_1 = 3.2$ km s^{-1}, *P*-wave velocity in uppermost layers;

V_i: *P*-wave velocity (in km s^{-1}) of seismic phases computed from raw data.

Travel-time corrections are less than 0.03 s and do not alter basically the main results.

P1 and P2 lines are reversed regarding shot and land station pattern. All shots were recorded at either station and so a seaward profile is available on both lines.

Discussion

Seismic records were digitized and are displayed as composite sections for P1 and P2 lines (Fig. 3a,b,c), whatever the shot location on each profile. As a first step, we assume a constant maximum amplitude for each of the seismic traces. Record sections will be further displayed (Fig. 8) taking into account variations in charge size and to make a partial allowance for geometrical spreading the amplitude has been scaled by $(W_0/W)^{0.64}$, where W is the shot weight and W is the reference weight, 25 kg (O'Brien 1960). Record sections have been band pass filtered from 2 to 20 Hz.

Despite the different shot points, calculations of *P*-wave velocities and intercept times for each shot demonstrate that the results inferred from composite sections were acceptable (correlation coefficient higher than 0.98). For ranges running from 10 to 40 km, we notice (Table 1), that *P*-wave velocities calculated by least square analysis using different figures are close to each other (standard deviation less than 0.15 km s^{-1}). A very simple error calculation shows that a 0.1 km s^{-1} change in velocity introduces a variation of about 0.2 s into the intercept times. Results from shot D on profile P1 differ slightly, the *P* velocity is comparable to those calculated from other shots, but the intercept time is greater than the mean value.

PLANE LAYER ANALYSIS

P-wave travel times for the two profiles P1 and P2 were first interpreted applying simple techniques, horizontal plane layers, and then used to define bounds on the velocity–depth function with the hypothesis that travel times are only range-dependent, whatever the shot

point on both profiles. We already noticed that correlation coefficients between travel time and range are always exceeding 0.98 for each seismic phase. Results from the preliminary study (Recq, Charvis & Hirn 1983; Charvis 1984; Recq & Charvis 1985) are summarized in Table 2.

Table 3 displays results assuming dipping layers. True velocities calculated from direct and reversed profiles introduce only gentle dips less than 3.5 per cent, but do not greatly affect the main results. Velocity–depth behaviour for P1 and P2 south (shots fired off Pointe Suzanne) resembles those published by Recq *et al.* (1983). On P2 north (shots fired

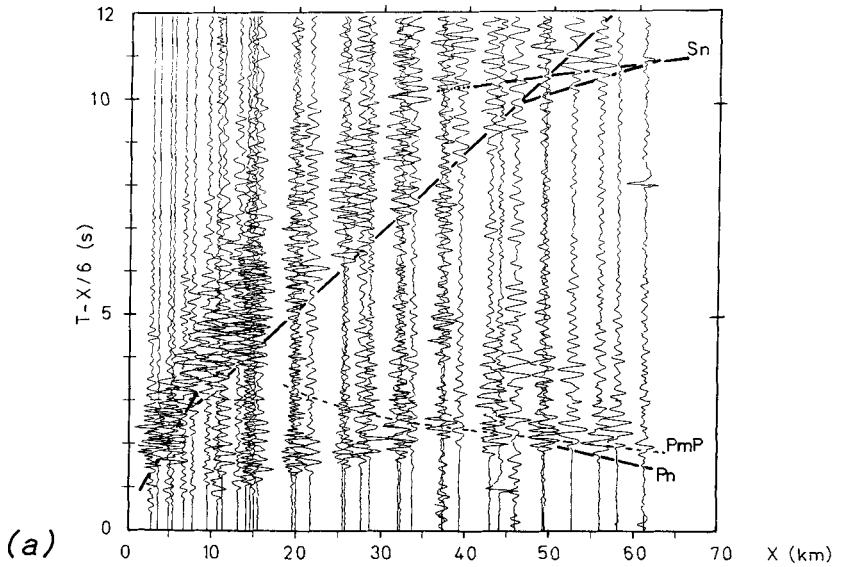

Figure 3. Composite record sections for P1 (a), P2 north (b) and P2 south (c). Travel times are reduced at 6 km s^{-1}. The traces have been band pass filtered from 2 to 20 Hz, and are plotted at equalized amplitudes. Shots were fired in the Baie du Hopeful on P2 north, and off Pointe Suzanne on P2 south. *Pn*-waves are recorded on P2 south as head waves at a range of only 45 km onward.

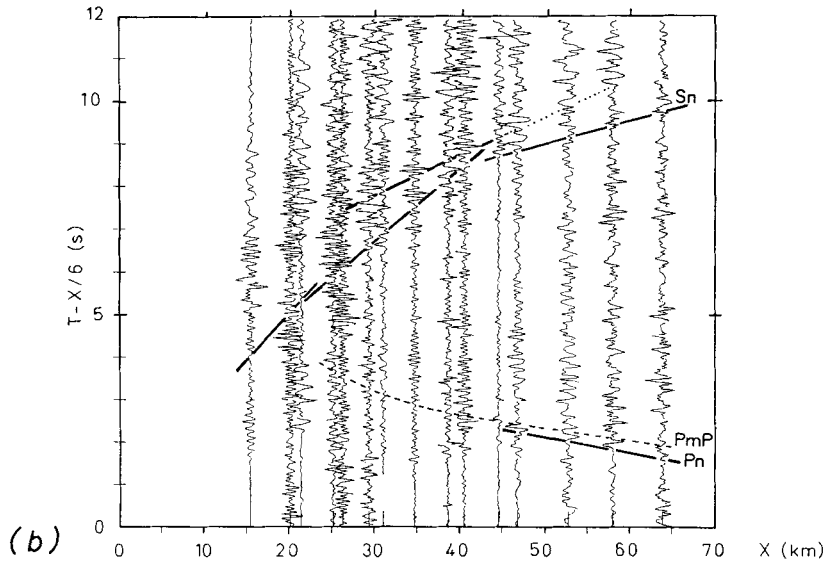

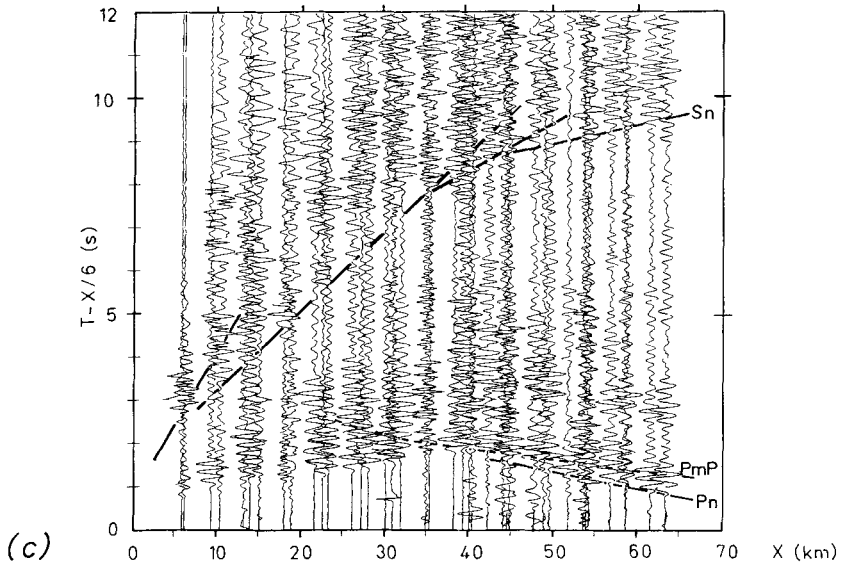

Figure 3 – *continued*

Table 1. *P*-wave velocities and intercept times calculated for ranges between 10 and 40 km, for each shot and the composite section as well.

Shot	A	B	C	D	Test shot	Mean value	Velocity from the composite section	Standard deviation
P1 Velocity eastward	4.90	4.94	5.01	5.23	5.06	5.03	5.03	0.13
Intercept time	0.25	0.54	0.58	0.97	0.65	0.60	0.59	0.26
P2 South northward	4.97	4.90	4.90	4.95	–	4.93	4.94	0.04
Intercept time	0.47	0.38	0.33	0.52	–	0.43	0.44	0.09

Table 2. Velocity–depth models inferred from preliminary studies (Recq *et al.* 1983).

Profile 1			Profile 2		
V	*h*	*H*	*V*	*h*	*H*
3.2	0.3	–	3.2	0.6	–
4.14	1.4	0.3	4.13	1.0	0.6
4.90	7.1	1.7	5.17	7.9	1.6
6.65	8.2	8.8	6.70	5.2	9.5
7.96	–	17.0	7.95	–	14.7

V (km s^{-1}): velocity; h (km): thickness; H (km): depth of interfaces.

in the Baie du Hopeful), no records have been made at ranges less than 12 km. Either the lack of records, or the presence of a deep discontinuity in the Baie du Hopeful, could partly explain the slight differences between results from P2 north and P2 south. Data from P2 south are the most reliable, owing to the quality (a very low background noise) and the number of seismograms. The profile P2 south is therefore regarded as the reference profile.

Table 3.

Range (km)	Intercept time (s)	Downward Velocity ($km\ s^{-1}$)		Upward velocity ($km\ s^{-1}$)	Dip > 0 for upward layer (per cent)	True velocity ($km\ s^{-1}$)
P1					Eastward	
0–9	0.12	4.03		4.27	−3.6	4.14
9–40	0.41	4.76		5.03	−3.3	4.89
40–60	2.35	6.46		6.87	−3.3	6.65
50–60	4.11	7.85		8.08	+2.2	7.96
P2 south					Northward	
0–10	0.23		4.13		0	4.13
10–36	0.43	4.93		5.12	−2.3	5.02
36–45	2.26	6.51		6.98	−3.9	6.73
45–65	3.55	7.80		8.11	+3.1	7.95
P2 north					Eastward	
15–20	0.03		3.71			
20–46	0.69		5.41			
25–50	2.22	6.75		6.83	−1.6	6.79
40–60	4.01		7.83			

On P1 and P2 south lines, the $3.2\ km\ s^{-1}$ layer is underlain by a 4.13 and $4.14\ km\ s^{-1}$ layer respectively. On the profile EL47–26 shot in the vicinity of the archipelago (Fig. 2), Houtz *et al.* (1977) observed a velocity of $4.15\ km\ s^{-1}$. The top of this layer could be related to the electrically conducting zone within the Plateau basalts of the Kerguelen Islands revealed by a magnetotelluric survey performed by Ballestracci, Nougier & Benderitter (1983). Data processing shows the presence of a conducting level parallel to the surface at 500–700 m depth, which roughly corresponds to the top of the $4.15\ km\ s^{-1}$ layer whose depth ranges from 300 to 600 m. According to Ballestracci *et al.* (1983), this magnetotelluric anomaly may be explained by a convection-type hydrothermal system.

Velocities of $4.15\ km\ s^{-1}$ would denote the existence of an altered basalt with a thickness up to 1 km. Palmason (1970) reported that a 1 km thick layer with an average velocity of $4.2\ km\ s^{-1}$ is found all over Iceland; in the Tertiary basalt districts, this layer is at the surface and underlain by a layer of average velocity of $5.1\ km\ s^{-1}$. The shallow velocity–depth behaviour is roughly the same in Kerguelen as in Iceland. The Courbet Peninsula is formed by horizontal basaltic strata (Nougier 1970). Most of the mobile stations were set up on Quaternary volcanic material predominantly basaltic.

Velocities of 4.89 and $5.02\ km\ s^{-1}$ are within the range of velocities in oceanic layer 2. Velocities of 6.65 and $6.73\ km\ s^{-1}$ recorded as first arrivals from 35 to 45–50 km range can be ascribed to velocities observed in oceanic layer 3.

The most striking features are *Pn*-waves recorded as first arrivals with a true velocity of $7.95\ km\ s^{-1}$ at a range less than 50 km in a subaerial domain. This visual observation on P2 south section (Fig. 3) and probably on the last two traces of P1 section suggests that the crust beneath the Kerguelen Isles and the Kerguelen–Heard Ridge is far thinner than that beneath a standard continental structure (30–40 km), where *Pn*-waves are recorded as first arrivals at a range of 160–180 km onward. Underneath P1, the average depth of the Moho discontinuity is down to 17 km (16 km below PAF), and only 14 km below the Val Studer on P2.

The thickening of the crust toward the centre of the archipelago is mainly caused by the change in the thickness of layer 3: from 5 km below PAF to 8 km thick towards Mont Ross.

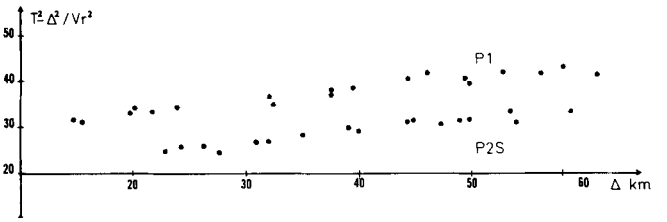

Figure 4. Reduced travel time–range plots for *PmP*-waves on P1 and P2 south, where T: travel time, Δ: range, V_r: reduced velocity of 6 km s^{-1}.

REFLECTED WAVES

The identification of reflected waves is rather difficult; only *PmP*-waves are displayed on the composite record section (Fig. 3). *PmP* travel-time curves were first studied using a T^2/X^2 plot where T is the travel time and X the range. In fact, Fig. 4 displays (T_r^2, X^2) plots, where $T_r = T^2 - X^2/V_r^2$, assuming a reduced velocity V_r of 6 km s^{-1}. Least squares straight lines were fitted to the data in order to compute the mean velocity within the crust on P1 and P2 lines.

Table 4.

Profile	Mean crustal velocity (km s^{-1})	Mean crustal thickness (km)
P1	5.69	16
P2	5.70	14

For each (T, X), the turning point of the reflected wave is assigned to an ellipse (X', h) whose equation is:

$$4(VT)^{-2}(X' - X/2)^2 + 4(V^2T^2 - X^2)^{-1} \cdot h^2 = 1$$

where

V: mean crustal velocity,

T: *PmP* travel time,

X: distance between the shot point to the station,

h: depth of the reflected layer at range X'.

On a profile, the shape of the reflected layer (Moho) is constructed from the envelope of the ellipses computed from (X, T) data (Fig. 5).

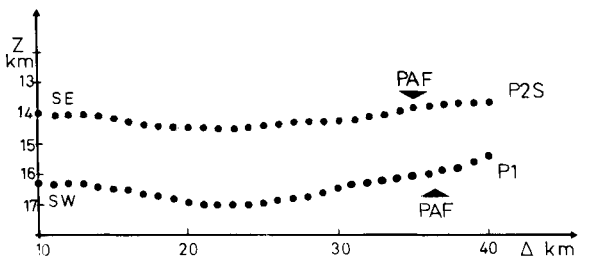

Figure 5. Moho depth on P1 and P2 south assuming a mean constant velocity of 5.70 km s^{-1} within the crust from the ellipse method. There is a discrepancy of 2 km between P1 and P2 in the vicinity of PAF. See the text for explanation.

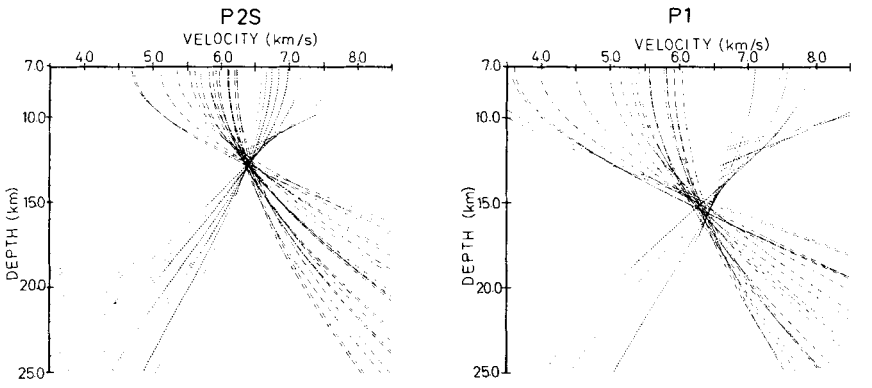

Figure 6. The Michel & Hirn (1980) procedure has been applied to *PmP* studies on profiles P1 and P2 south. The influence of shallow layers has been removed by using seismic refraction data. The average velocity within layer 3 is of the order of 6.50 km s^{-1}.

PmP travel times were afterwards studied by Michel & Hirn's (1980) procedure. The observed travel-time curves of a reflected wave are corrected for the influence of all such known or estimated structures, down to the top of the layer the base of which is the reflector; the depth Z_0 and the mean velocity V_0 of this layer are computed. This method is also suitable with dipping interfaces. Fig. 6 displays results dealing with profiles P1 and P2 south.

The average crustal thickness calculated from *PmP* wave studies is 16 km below P1 and 14 km below P2 (12 km below the Val Studer). The mean velocity within layer 3 computed using Michel & Hirn's (1980) procedure is 6.50 km s^{-1} on both lines.

The crust is thinning towards the Australia–Antarctic Basin. Inspection of the P2 south data suggests important changes into the Moho dip which are consistent with gravity anomalies through the Val Studer.

The progressive transition between layers 2 and 3 (Fig. 3) explains the lack of reflected waves on crustal interfaces and the poorly determined velocity of layer 3 on P2 south.

RAY TRACING

A ray tracing method was applied at IPGP. Travel times derived from ray tracing match well those observed on record sections (Fig. 3). The top of layer 2 is roughly 1 km deep, below 3.2 and 4.13 km^{-1} velocity layers on both lines. Within layer 3, the *P* velocity increases from 6.3 to 6.8 km s^{-1} on P1, and from 6.3 to 7 km s^{-1} on P2. The mean depth of the Moho is at 16 km below P1 and 13 below P2. On both lines, the crust is thinning toward the Australia–Antarctic Basin as already observed from *PmP* wave studies. On P2 south line, the Moho is 15 km deep in the vicinity of PAF; this maximum value being in accordance with gravity data (Fig. 11). The *Pn* velocity, 7.96 km s^{-1}, is lower than that determined by Francis & Raitt (1967) and by Recq & Goslin (1981), 8.11–8.08 km s^{-1} for the southern Indian Ocean.

The positive velocity gradient within layer 2 and the boundary between layers 2 and 3 modelled only by a change in the velocity gradient (Fig. 7) may explain the poorly determined layer 3 velocity on P2 south line. The Moho may be modelled either by a first-order discontinuity, or by a progressive transition by means of a velocity gradient; this latter figure could explain the low amplitudes of *PmP*-waves.

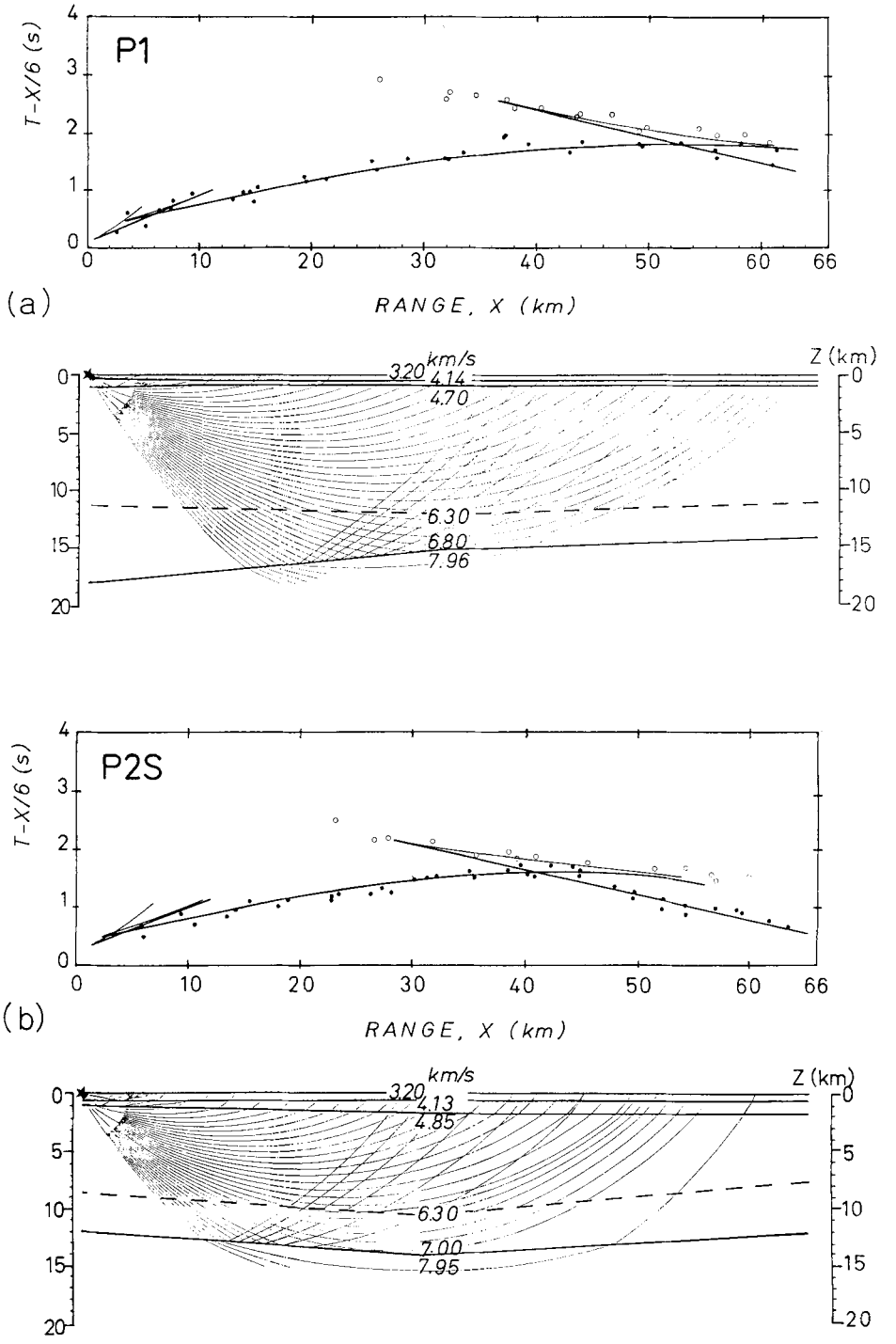

Figure 7. Examples of results obtained by ray-tracing showing observed and modelled arrivals on P1 (a) and P2 south (b), assuming positive gravity gradients within the crust. The upper diagrams show comparisons of observed travel times (dots and open circles) and calculated travel times denoted by solid lines. The lower diagrams show the velocity models and the ray diagrams.

SYNTHETIC SEISMOGRAMS

Synthetic seismograms for P1 and P2 south lines were calculated at Bullard Laboratories by PC with the assistance of George Spence and Martin Sinha. Methods were developed by Chapman & Drummond (1982) from the asymptotic ray theory for the computation of body wave seismograms. Synthetic seismograms were computed with the assumption that

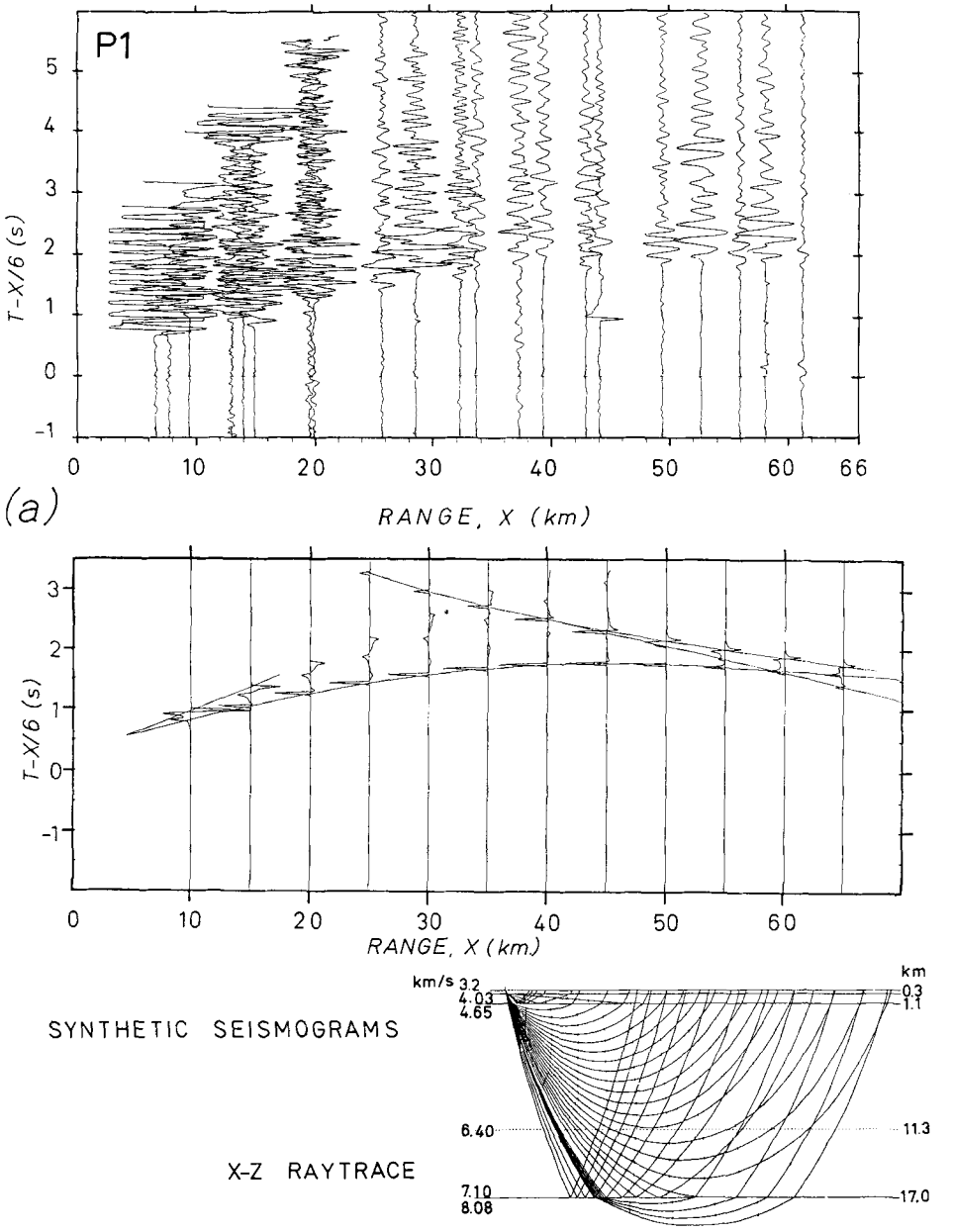

Figure 8. Comparison of the observed record section with synthetic seismograms calculated using the velocity–depth function shown on ray-tracing models for P1 (a) and P2 south (b) lines. The observed seismograms were scaled for charge weight. The synthetic seismograms were calculated using the Chapman & Drummond (1982) procedure.

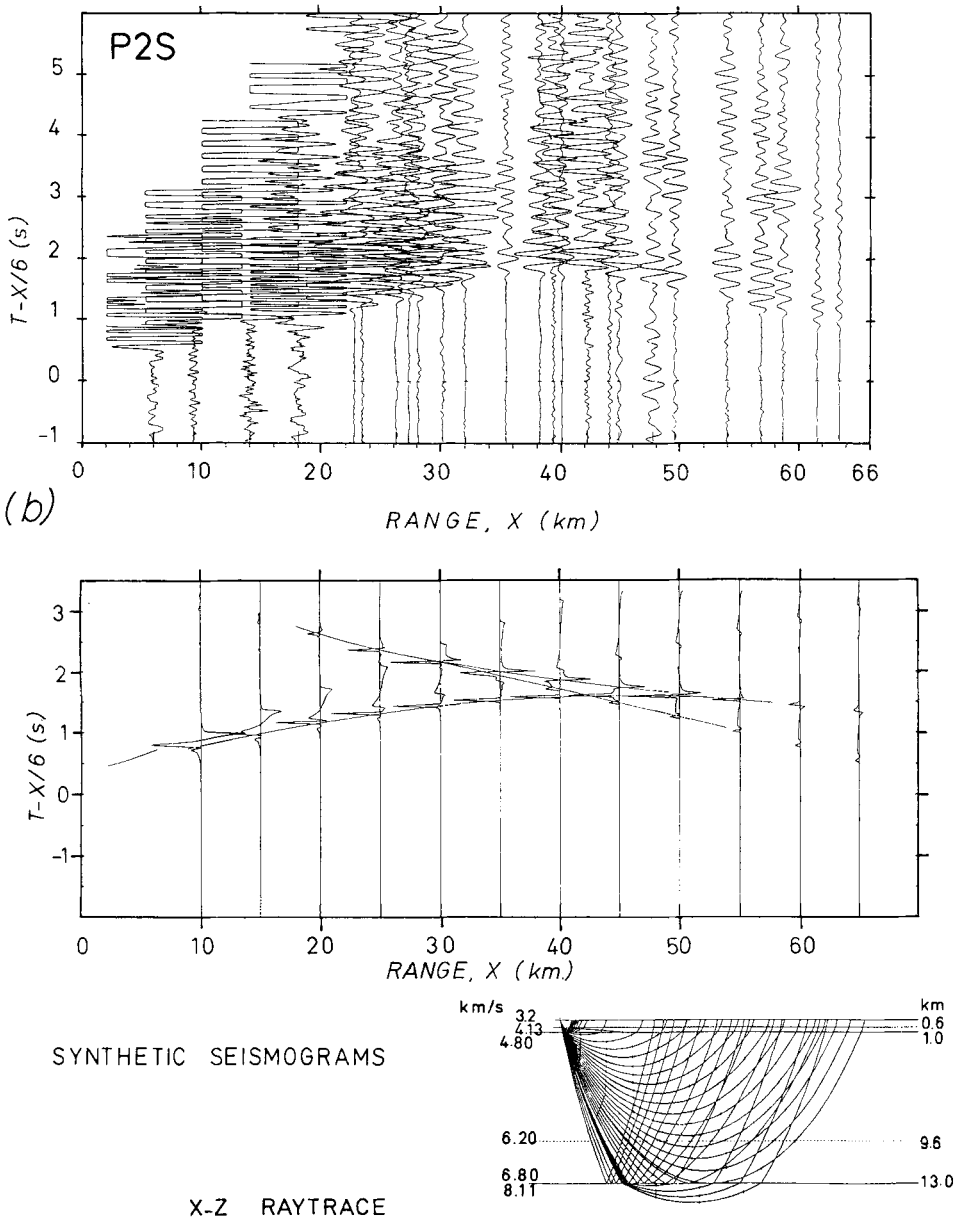

Figure 8 – *continued*

velocity is only depth dependent; this implies that structure beneath Kerguelen is modelled from apparent velocities on P1 and P2 lines. Velocity–depth functions inferred from synthetic seismograms slightly differ from those calculated using ray tracing methods.

The best fitting models are shown on Fig. 8. A sedimentary layer of 0.3 km thick on P1, and 0.6 km on P2 with the assumed velocity $V = 3.2\,\mathrm{km\,s^{-1}}$ overlays an altered basalt layer with a velocity of $4.03\,\mathrm{km\,s^{-1}}$ on P1 line, and $4.13\,\mathrm{km\,s^{-1}}$ on P2 line (0.8 km thick beneath P1 and 0.4 km thick beneath P2); then, a steep velocity gradient of $0.16\,\mathrm{s^{-1}}$ on both profiles, from 4.65 to $6.40\,\mathrm{km\,s^{-1}}$ on P1 and from 4.80 to $6.0\,\mathrm{km\,s^{-1}}$ on P2, extends to a

depth of 11.3 km on P1 and 9.6 km on P2. In the lower crust, velocities increase from 6.40 to 7.10 km s^{-1} on P1 and from 6.2 to 6.8 km s^{-1} on P2 down to the Moho interface which is 17 km deep below P1 and 13 km deep below P2.

To allow comparison between synthetic seismograms and record sections, amplitudes have been scaled, as already noticed, by the factor of $(W_0/W)^{0.64}$ (O'Brien 1960), where W is the shot weight and W_0 the 25 kg charge. Despite scaling, heterogeneities in amplitudes are still persisting which do not allow an accurate comparison between observed and computed record sections. Nevertheless, modelling allowed us to compute an amplitude–range behaviour of first arrivals and *PmP*-waves alike to those observed on P1 and P2 lines. As stated above, it is essential that the transition between layers 2 and 3 has to be modelled rather by a change into the velocity gradient than by a discrete interface.

The velocity of 6.2–6.3 km s^{-1} is commonly observed at the base of layer 2 within oceanic regions located near spreading ridges and fracture zones (White & Purdy 1983; Sinha & Louden 1983). Bunch & Kennett (1980), from synthetic seismograms, suggested that the 5.4–6.2 km s^{-1} layer observed beneath the Reykjanes Ridge may be a region of velocity gradient rather than a constant velocity layer; for these authors, it is unlikely that there is a sharp boundary between the basaltic layer 2 and higher velocity layer 3 rocks.

S-WAVE ANALYSIS

Well developed *S*-waves are clearly displayed on seismic record sections P1, P2 south and P2 north (Fig. 3). Charges detonating either near or on the sea bottom allow efficient coupling between the seismic source and the seabed.

S-wave analysis has been performed using horizontal components and sometimes, in case of failure, the vertical component. Straight lines were fitted by least squares to travel-time segments. The Poisson' ratio σ has been calculated from the following formula:

$$\sigma = \tfrac{1}{2}\left[\left[1 - \left[(V_p/V_s)^2 - 1\right]^{-1}\right]\right],$$

whereas V_p and V_s are respectively *P*- and *S*-wave velocities.

Results are summarized in Table 5.

Table 5.

	P1				P2 south				P2 north			
Range	0–10	10–53	32–62	37–62	0–10	10–36	31–45	45–64	15–22	21–41	31–41	38–6
V_p	4.14	4.89	6.65	7.96	4.13	5.03	6.73	7.95	3.71*	5.41*	6.79	7.83
V_s	2.42	2.84	3.31	4.25	2.01*	2.63	3.45	4.42	2.10*	3.17*	3.76*	4.22
σ	0.24	0.25	0.34	0.30	0.34	0.31	0.32	0.28	0.26	0.24	0.28	0.30

* Apparent velocity.

The Poisson's ratio is related to the nature of material and gets higher values for alkaline rocks than for acid material: 0.30 for gabbros and 0.25 for granites (Christensen & Salisbury 1975).

Most of the Poisson's ratios for layer 2 are lower than those determined by Spudich & Orcutt (1980) for a 15 Myr old crust in the Pacific Ocean near Guadalupe Island off Baja California (Fig. 9). According to these authors, σ would be lowered either by addition of cracks and the pore effect, or by an age-related phenomenon.

On the other hand, the average value of σ inferred from our data for layer 3 is of 0.31, which is slightly higher than those given by White (1979) and Purdy (1983) for a

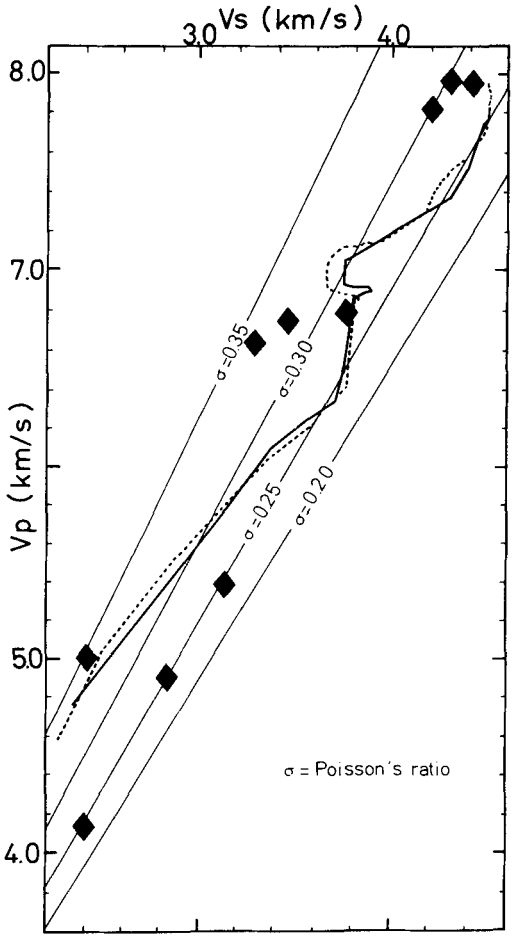

Figure 9. Comparison of the observed Poisson's ratio–depth behaviour in Kerguelen with that computed for a 15 Myr old oceanic crust from two seismic profiles FF2 (solid lines) and FF4 (dotted lines) carried out in the Pacific Ocean by Spudich & Orcutt (1980).

110–140 Myr old crust in the Atlantic Ocean, and (Fig. 9) by Spudich & Orcutt (1980), but close to that calculated for the lower part of layer 3 near the Atlantic Ridge (Fowler 1976).

High amplitude of *S*-waves on our profiles precludes either a partial melting zone, or magma chambers within the crust below the Courbet Peninsula.

Gravity studies over the Kerguelen Isles and the Kerguelen–Gaussberg ridge

(I) THE KERGUELEN ISLES

A gravity survey was conducted in 1962 by Gaston Rouillon from the Expéditions Polaires Françaises in the Kerguelen Isles, using a Worden gravimeter that has been previously calibrated in France and Réunion Island. The data set (114 stations) collected throughout the archipelago, excluding the westernmost margin and the Rallier du Baty Peninsula, was connected to the world-wide network through the station Martin at Port des Galets (Réunion). A Bouguer gravity anomaly map over Kerguelen was drawn by Rouillon (1963),

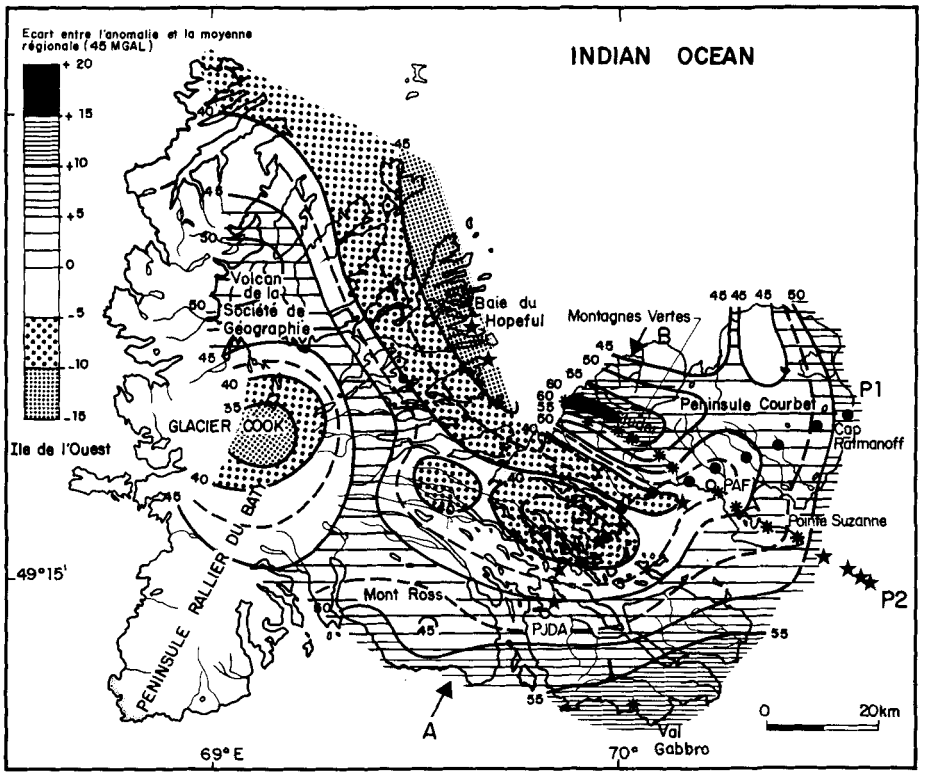

Figure 10. Unpublished gravity contours relative to the regional mean value of the Bouguer anomaly (+45 mgal), after Rouillon (1963). The assumed mean crustal density was 2.67 g cm^{-3}. The contour interval is 5 mgal. Intermediate contours are marked by dashed lines.

the influence of the topography being removed. This document stored (Fig. 10) in TAAF archives has never been published. A 2′ x 2′ grid over the Kerguelen Isles was constructed in order to compute topographical corrections and Bouguer anomalies. The mean elevation of the Kerguelen Isles is 250 m. Bouguer anomalies were calculated by Rouillon and Helly assuming a crustal mean density of 2.67 g cm^{-3}; this mean crustal value has been confirmed by refraction work, but does not preclude any local inhomogeneities within the crust. The average free air and Bouguer anomalies respectively are +50 and +45 mgal relative to the IGSN 71 system. The latter values are rather low, compared to those calculated for oceanic features such as: the Hawaii Island, + 240 mgal (Kinoshita *et al.* 1963; Ryall & Bennett 1968; Zucca *et al.* 1982), the Hawaiian Emperor Seamount Chain, +250 mgal (Watts & Cochran 1974), the Ninetyeast Ridge, +300 mgal (Bowin 1973), the Galapagos Islands, +100 mgal (Case *et al.* 1973), the Réunion Island, + 220 mgal (Gérard *et al.* 1980).

The average free air anomaly over the Kerguelen Isles (excluding the Glacier Cook and the westernmost margin of the main island) is close to that determined by Houtz *et al.* (1977) over the Kerguelen–Gaussberg surrounding deep basins. This similarity indicates a near local isostatic compensation of the Kerguelen Isles and the Kerguelen–Heard Ridge.

A preliminary inspection of the data reveals that Bouguer gravity anomalies with respect to the average value range only from −15 to +15 mgal. The steepest anomaly is located across the Val Studer tectonic trench (Fig. 10) along the north-eastern margin. The Bouguer anomaly is down to −13 mgal and up to +15 mgal along the Courbet Peninsula margin. So

there is a gravity 'jump' somewhere south of the Golfe des Baleiniers, in the Baie du Hillsborough, off the northern end of Val Studer. This jump could be related to the assumed crustal discontinuity suggested by seismic results located there. A negative anomaly, less than −15 mgal, is observed over Glacier Cook. A local Moho deepening caused by the glacial overload may be responsible for this anomaly. However, Rouillon, in an attempt to calculate the mean density of rocks below the glacier, found a density ranging from 2.3 to 2.5 g cm^{-3} (private communication). It is difficult to ascertain whether this hypothesis is valid as the crustal structure beneath the glacier is not controlled by refraction seismic data. Some important features with regard to the extent of the Kerguelen Isles, such as Mont Ross (1852 m), the Société Géographicque volcanic massif (1000 m) (Fig. 2) only display short-wavelength gravity anomalies less than − 5 mgal. The compensation of these young features aged 1 Myr or less is achieved by local shallow inhomogeneities within the crust.

SW of the Kerguelen Isles, a +10 to +15 mgal anomaly is displayed over the south-eastern end of the Presqu'île Jeanne d'Arc (Figs 2 and 12). This positive anomaly suggests the presence of shallow high density material; the exposed plutonic complex in Val Gabbro (Fig. 2) supports this latter hypothesis.

A very simple calculation demonstrates that short-wavelength steep anomalies, up to 20 km, are not modelled by abrupt changes in the Moho depth. Moho undulations originate only long-wavelength (over than 20 km) Bouguer anomalies. By using Dobrin's (1976) procedure, gravity anomalies were modelled in terms of laterally-varying crustal model along the profile and compared to seismic crustal models. The density of crustal layers was determined from seismic velocities by Ludwig, Nafe & Drake's (1970) law.

On profile P1 (Fig. 11), west of PAF, gravity anomalies may be interpreted mostly by Moho undulations, and toward Cap Ratmanoff, NE of Courbet Peninsula, as a crustal thinning to 14 km. Moho undulations cannot explain the observed anomaly gradient near Mont Ross. The short wavelength of the − 5 mgal anomaly on Mont Ross indicates that this anomaly is generated at shallow depth by low density material, 2.3 g cm^{-3} as shown on Fig. 11. Mont Ross has no downward extension and appears to be constituted by lower densities than the surrounding areas.

The gravity model on profile P2 (Fig. 11) shows the Moho at depth beneath PAF, in close agreement with the refraction results indicating a 14 km deep Moho in this region. The crust thins toward either end of the profile, Baie du Hillsborough and Pointe Suzanne (Fig. 12). Beneath the Val Studer, the steep gravity gradient could suggest a rapid uplift seen from wide-angle reflection data. This figure does not fully explain the origin of this gravity gradient.

The gravity profile AB across the Val Studer (Fig. 11) shows very steep gravity gradients, 20 mgal per 10 km, with a maximum anomaly width of 3 km. This narrow anomaly cannot be modelled by abrupt changes in the Moho depth and may have originated by a 3.0 g cm^{-3} density, intrusive body as depicted in Fig. 11, which is interpreted as a near vertical dyke system of magmatic rocks related to faults, edging the Val Studer trench and to the Montagnes Vertes plutonic complex nearby (Fig. 12).

Modelling crustal structure leads to an average Moho depth of 16–17 km below P1 and 13–14 below P2. However, wide-angle reflection and dipping layer model studies point out that, west of PAF, where the two profiles cross almost at right angles, the discrepancies are roughly of 2 km. Two kinds of explanation may be put forward: (1) after Nougier (1970), the easternmost part of the Courbet Peninsula has collapsed, this region is bounded to the east by a major fault (Fig. 12), orientated NNE–SSW, that may affect the entire crust and probably the Moho; (2) gravity models for P2 and AB lines (Fig. 11) are consistent with the presence of high density intrusive plutons below the Val Studer near the Montagnes Vertes. *PmP*-waves are recorded on receivers set up in the Val Studer, so the upward reflected wave

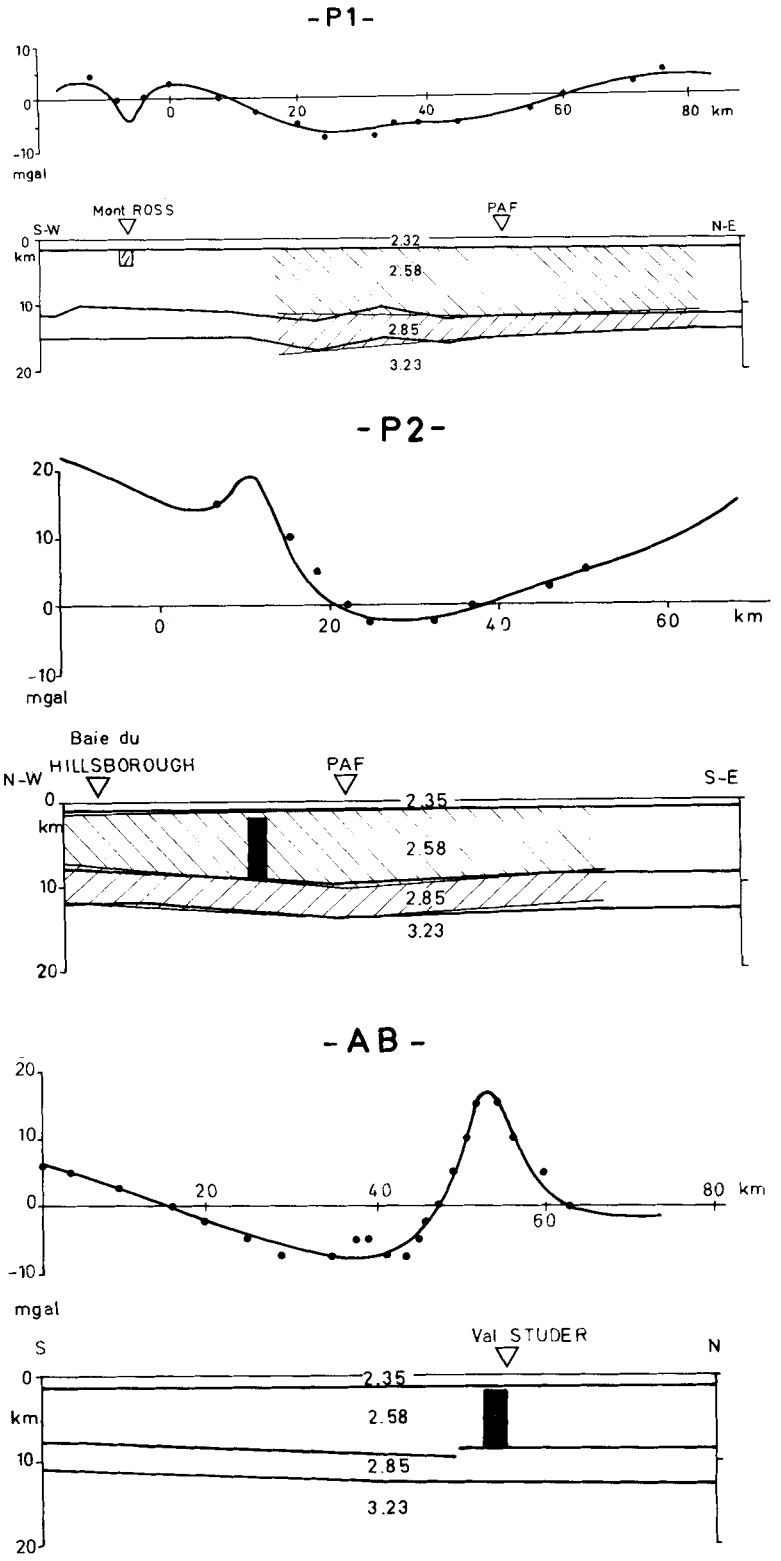
-P1-
10
0
-10
mgal
0
20
40
60
80 km
Mont ROSS
PAF
S-W
N-E
0
km
10
20
2.32
2.58
2.85
3.23
-P2-
20
10
0
-10
mgal
0
20
40
60
km
Baie du
HILLSBOROUGH
PAF
N-W
S-E
0
km
10
20
2.35
2.58
2.85
3.23
-AB-
20
10
0
-10
mgal
20
40
60
80 km
Val STUDER
S
N
0
km
10
20
2.35
2.58
2.85
3.23

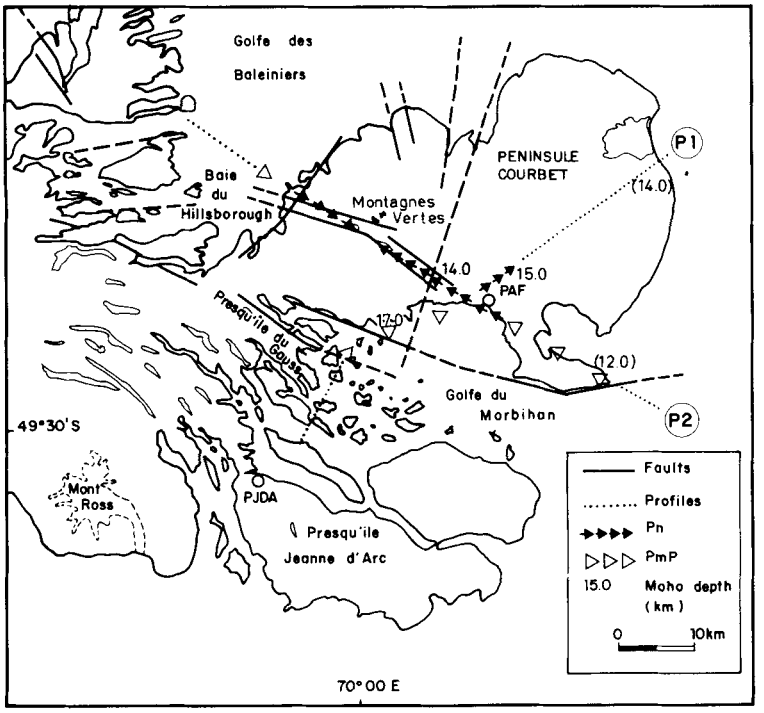

Figure 12. Map of the investigated region showing the fault system depicted by Nougier (1970) and Giret (1983). Moho depths in kilometres calculated from refraction and reflection data are also plotted.

propagates through a high velocity intrusive body as suggested by gravity modelling. The presence of this intrusive body shortens the upward reflected wave travel time. To keep the travel time assigned to shot and receiver constant, the Moho interface has to be lowered in order to increase the incident wave travel time.

(II) THE KERGUELEN–GAUSSBERG RIDGE

On the Kerguelen–Gaussberg Ridge, gravity data are scarce. The profile A-A′ (Fig. 13) of Houtz *et al.* (1977), orientated NE–SW, traverses the Kerguelen–Gaussberg Ridge between latitudes 56 and 60°S, at a great range southward from the archipelago. According to these authors, although the local variations in the free air anomaly are large, the mean level of these anomalies is positive throughout the region; the oceanic basins show positive anomalies of the order of +15 to +25 mgal, and the average level of anomalies over the Kerguelen–Gaussberg Ridge is about +40 mgal. If the Kerguelen–Gaussberg Ridge represents an entirely uncompensated block of oceanic extrusives sitting on an otherwise 'normal' oceanic crust,

Figure 11. Bouguer gravity profiles along P1, P2 seismic lines, and the AB line crossing the Val Studer at right angles (see Fig. 10 for location). Dots indicate observed gravity anomaly on each of the profiles. Solid lines show the computed anomaly assuming laterally varying structures. Crustal models inferred from seismic data (hatched) match gravity models on P1 and P2 lines. The steep anomaly displayed on profile AB is modelled by the shaded intrusive body with a density of 3.0 g cm^{-3} also shown on P2 line below the Val Studer. The short-wavelength anomaly beneath Mont Ross is modelled by a shallow low density (2.3 g cm^{-3}) body located within the volcano. No crustal root appears to be present below Mont Ross.

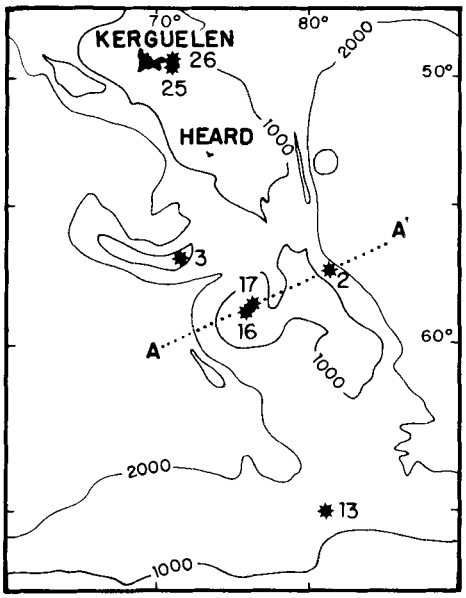

Figure 13. Simplified map of the Kerguelen–Gaussberg Ridge showing the gravity profile AA' and the sonobuoys stations implemented during the *R/V Eltanin* cruise (Houtz *et al.* 1977). Bathymetric contours are in metres.

the gravity anomalies over the ridge would be approximately +200 mgal relative to the oceanic basins values. Houtz *et al.* (1977) consider that the absence of long wavelength anomalies, and the low values of the positive anomalies indicate that the Kerguelen–Gaussberg Ridge is nearly compensated and the compensation is achieved by an unextended low density beneath the ridge. According to these authors, the compensation might be achieved by a crustal root 10 km thicker than the oceanic crust; this implies a total thickness of the crust of 23 km. They did not preclude the presence of a low density zone within the upper mantle beneath the Kerguelen–Gaussberg Ridge to explain the low free air gravity anomalies.

Results inferred from the first deep seismic soundings in the Kerguelen Isles invalidate the hypothesis of Houtz *et al.* (1977) postulating the existence of a 10 km thick crustal root beneath the Kerguelen–Gaussberg Ridge. The average thickness of the crust is only 16 km. This implies a 3–4 km thicker crust beneath the ridge than in nearby oceanic basins. This thickness is inadequate to explain the observed gravity anomalies.

All early available refraction data relating to the deep structure of features located in the southern Indian Ocean were compiled. Hales & Nation (1973), Recq & Goslin (1981), Sinha, Louden & Parsons (1981) and Recq (1983), from refraction data converted into densities, have shown that most of the aseismic ridges, including the Crozet Rise, are locally compensated. However, the southern domain of the Madagascar Ridge is uncompensated and is undergoing subsidence. This study has been updated, taking Kerguelen data into account. The weight A of a column of material, with a constant section is calculated for every aseismic ridge in the southern Indian Ocean, including the continental Seychelles and the aseismic Saya de Malha Banks, the Crozet Basin, but excluding all data on spreading ridges. The greatest depth to the Moho discontinuity in the southern Indian Ocean is 32 km below sea-level, beneath the Seychelles Bank (Matthews & Davies 1966). This is chosen as a reference level.

In fact, A is calculated using the following formula:

$$A = \rho_0 h_0 + \Sigma \rho_i h_i + (32 - M)\rho_m,$$

where

h_0: the water depth (in km);

ρ_0: the density of seawater, $\rho_0 = 1.03\ g\ cm^{-3}$;

h_c: the crustal thickness (in km);

h_i: the thickness (in km) of the layer i, the density of which is ρ_i;

M: the Moho depth (in km), $M = h_0 + \Sigma h_i$;

ρ_m: the upper mantle mean density (in $g\ cm^{-3}$), $\rho_m = 3.31\ g\ cm^{-3}$ (Recq 1983).

Inspection of data compiled in Table 5 shows that:

(a) Kerguelen resembles the submerged Crozet Rise; beneath Kerguelen, $h_c = 16$–17 km; beneath Crozet, $h_c = 16$ km;

(b) the mean density of the crust is almost the same for both structures, Crozet, $\rho_c = 2.68\ g\ cm^{-3}$, Kerguelen, $\rho_c = 2.67\ g\ cm^{-3}$;

(c) assuming a constant upper mantle density throughout the southern Indian Ocean, the Crozet Rise, but not the Kerguelen–Heard Ridge, is compensated with respect to the Crozet Basin.

This last statement is inconsistent with gravity data collected over the Kerguelen–Gaussberg Ridge by Houtz *et al.* (1977) that indicate a nearly achieved local compensation. These authors postulated a constant mean upper mantle density underneath the Crozet Basin and the Kerguelen–Gaussberg Ridge; however, this assumption appears to be invalidated by *Pn* velocity studies. Upper mantle velocities in the Crozet Basin calculated by Francis & Raitt (1967) are higher, up to $8.39\ km\ s^{-1}$, than the average subcrustal velocity for the southern Indian Ocean, $8.11\ km\ s^{-1}$ (Francis & Raitt 1967). According to these authors, *Pn* velocities in the Crozet Basin are lower, $7.99\ km\ s^{-1}$, toward the SE Indian Ridge. This value is almost the same as that determined for the Kerguelen Isles, $7.96\ km\ s^{-1}$.

Fig. 14 shows the (h_0, h_c) behaviour, where h_0 is the water depth and h_c the thickness of the crust related to features listed in Table 6. We note that the plotted (h_0, h_c), except for S2 on the southern Madagascar Ridge and Kerguelen (KER), are distributed along two distinct lines according to the mean density ρ_c of the crust; line I for structures, the density of which is close to $2.80\ g\ cm^{-3}$ (group I), and line II for densities close to $2.70\ g\ cm^{-3}$ (group II). Using least squares analysis, $h_c = -5.59 h_0 + 32.65$ (line I), and $h_c = -3.98 h_0 + 23.38$ (line II). The mean density of the crust related to thick ridges (group I) is higher than that related to thin ones (group II). Both the structures plotted on lines I and II are respectively in local isostatic equilibrium according to Airy's hypothesis. The mean density of the crust beneath Kerguelen, $2.68\ g\ cm^{-3}$, is the same as those densities in group II. Putting $h_0 = 0$ into formula II, $h_c = 23.4$ km. Refraction studies do not support the existence of a 23 km deep crustal root beneath the ridge and invalidate the hypothesis of Houtz *et al.* (1977). Low *Pn* velocities, $7.95\ km\ s^{-1}$, below the mean *Pn* velocity of $8.11\ km\ s^{-1}$, throughout the southern Indian Ocean, enhance the hypothesis for a participation of the mantle into the compensation of the ridge. The low positive free air anomalies may indicate the Kerguelen–Heard Ridge is undergoing subsidence.

Table 6.

Profile	h_0	h_c	M	ρ_c	A	Group	Reference
Ninety East Ridge							
40	3.75	8.22	11.97	2.81	93.2	I	Francis & Raitt (1967)
Madagascar Ridge							
N1 north	2.60	20.56	22.56	2.85	91.7	I	Recq *et al.* (1979)
N1 south	2.20	22.20	24.40	2.89	91.8	I	Sinha *et al.* (1981)
S2 south	1.30	13.44	14.74	2.68	94.5		Recq *et al.* (1979)
Mozambique Ridge							
H13	3.50	11.00	14.50	2.61	90.2	II	Hales & Nation (1973)
H14	2.40	19.76	22.16	2.81	90.5	I	Hales & Nation (1973)
H15	1.50	23.76	25.26	2.82	92.2	I	Hales & Nation (1973) and
H16	2.50	18.01	20.51	2.76	90.3	O	Recq & Goslin (1981)
Agulhas Plateau							
B9	3.00	12.36	15.36	2.61	90.2	II	Barrett (1977)
L150	3.84	9.55	13.49	2.69	91.2	II	Ludwig *et al.* (1968)
Crozet Rise							
MD5-16	1.90	15.60	17.50	2.69	91.9	II	Goslin *et al.* (1981a)
Kerguelen Isles							
P1	0	17.0	17.0	2.67	95.0		Recq *et al.* (1983) and this
P2	0	14.7	14.7	2.67	96.5		paper
Broken Ridge							
42	1.97	21.60	23.55	2.88	90.2	I	Francis & Raitt (1967)
42–43	1.97	18.30	20.27	2.79	92.2	I	Francis & Raitt (1967)
Seychelles Bank							
SB	0.05	31.95	32.00	2.82	90.2	I	Matthews & Davies (1966)
17–18	3.98	6.35	10.33	2.71	93.0	II	Francis & Shor (1966)
Saya de Malha Bank							
22–23	3.96	5.70	9.66	2.70	93.4	II	Francis & Shor (1966)
23–24	3.98	5.64	9.62	2.61	92.9	II	Francis & Shor (1966)
25–26	3.15	13.81	16.96	2.68	90.0	II	Francis & Shor (1966)
Crozet Basin off ridges							
34	4.79	6.12	11.91	2.81	92.0	I	Francis & Raitt (1967)
34–35	4.82	5.73	10.55	2.69	91.4	II	Francis & Raitt (1967)
36	4.99	4.42	9.41	2.77	92.2	I	Francis & Raitt (1967)

The average $\bar{A}$ value is 91.6 ± 1.1, excluding P1, P2 and S2.
Group I $\overline{\rho_c}$ = 2.82 ± 0.04 g cm^{-3}.
Group II $\overline{\rho_c}$ = 2.68 ± 0.04 g cm^{-3}.

The oceanic origin of the Kerguelen–Heard Ridge

Recent geological investigations in the Kerguelen Isles, mostly in the intrusive complex of the Rallier du Baty Peninsula, SW of the archipelago (Fig. 2) preclude a continental origin of the ridge. No evidence suggests that these islands are fragments of a continent, no sample from continental basement has been discovered, either in plutons, within lava, or in ejecta (Watkins *et al.* 1974; Marot & Zimine 1976; Lameyre *et al.* 1976; Giret 1980, 1983). Watkins *et al.* (1974) pointed out a continuous petrochemical series between quartz and basanite, and also between rhyolite and phonolite similar to those observed in oceanic islands. The maximum isotopic age determined for these lavas ranges from 24 to 27 Ma, less than that of

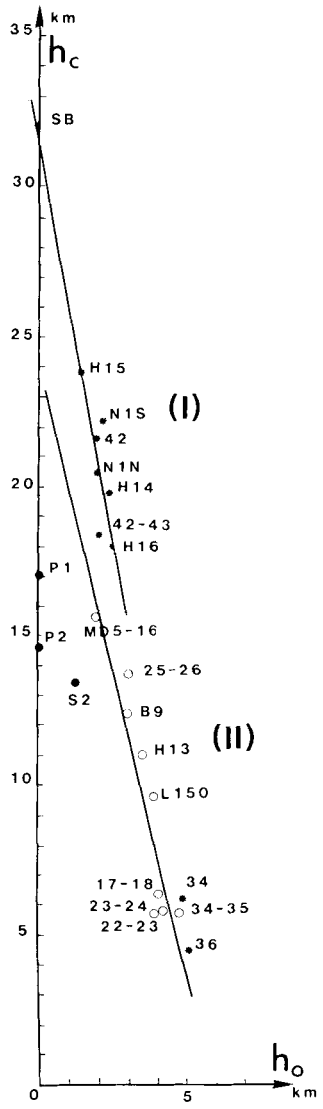

Figure 14. Crustal thickness h_c – water depth h_o function from refraction studies for aseismic ridges compiled in Table 5, the continental Seychelles Bank and the Crozet Basin being added for comparison. We notice that these features are distributed into two lines, according to their mean crustal density. S2 (southern domain of the Madagascar Ridge), P1 and P2 do not coincide with either of these two distinct groups. The mismatch of P1 and P2 shows that the near isostasy of the Kerguelen–Heard Ridge is not achieved by Airy compensation.

31–45 Ma to the north and NE of the Kerguelen–Heard Ridge, calculated from the seafloor magnetic anomaly pattern (Schlich & Patriat 1971; Schlich 1975, 1983; Houtz *et al.* 1977; Patriat 1983). The discovery in Val Gabbro (Péninsule Jeanne d'Arc) of a tholeiitic transitional complex at least as old as 39 Ma shows agreement with the oceanic linear anomalies and the geochronological data.

Although some measurements from volcanic rocks collected in Kerguelen provide $^{87}Sr/^{86}Sr$ higher and $^{143}Nd/^{144}Nd$ lower than those observed in oceanic basalts, according to Dosso &

Murthy (1980), the data preclude an involvement of old continental crust in the genesis of granites and syenites, and support the hypothesis that the source of Kerguelen plutonic and volcanic rocks could be located within an enriched mantle with a higher Rb/Sr ratio, and a lower Sm/Nd ratio than within the bulk Earth. In oceanic regions, the mantle has undergone a partial melting at the spreading ridge at some earlier time, when the lithosphere has been emplaced. The reservoir would lie beneath the depleted oceanic upper mantle. These assumptions are compatible with a convective system within the mantle.

Dupré & Allègre (1983) noticed that the isotopic ratios from Indian Ocean ridges and islands differ from these calculated for the Pacific and the North Atlantic oceans. These observations led these authors to consider that the lower mantle could be contaminated by reinjection of sediments. This enriched domain may contaminate the hot spots when they rise toward the surface. According to McKenzie & O'Nions (1983), the mantle part of the continental lithosphere possesses in part Sr and Nd isotopic compositions similar to those of ocean island basalt. Mantle material may become detached from continental lithosphere, be incorporated into the convective flow and thereby provides a source for some ocean island basalts.

Results outlined from this preliminary refraction work in the Kerguelen archipelago enable us to invoke an oceanic-type structure at least in the northern domain of the Kerguelen–Gaussberg Ridge. The crustal thickness and the velocity–depth behaviour resemble those calculated for the Crozet Rise and the Madagascar Ridge, the oceanic origin of which is now well ascertained (Recq *et al.* 1979; Goslin *et al.* 1981a; Sinha *et al.* 1981).

Average velocities of 5.5 and 6.6 km s^{-1} are in the range of those observed respectively in oceanic layers 2 and 3. The transition to mantle velocities modelled as a zone of positive velocity gradient occurs frequently within oceanic structures generated near spreading centres, such as the Reykjanes Ridge (Bunch & Kennett 1980), the North Atlantic Ridge (Fowler 1978; White & Purdy 1983; Sinha & Louden 1983), and the East Pacific Rise (Orcutt, Kennett & Dorman 1976; Spudich & Orcutt 1980). Comparing the structure of the crust beneath the Kerguelen Isles with a typical oceanic crust, we note that the thickness of layer 2, up to 2 or 3 km for a standard model, increases to 8 to 9 km beneath Kerguelen. So the crustal thickening toward the Kerguelen Ridge is mainly within layer 2, caused by stacking of tholeiitic basalt layers recognized on land (Watkins *et al.* 1974) or dredged over the ridge (Ewing *et al.* 1972).

Velocities of 4.7–4.85 km s^{-1}, at the top of layer 2 can be ascribed to a low density or a highly fracture basalt. According to Stephen (1978), a basalt with 11 per cent porosity would have a velocity of 4.8 km s^{-1}. Houtz *et al.* (1977), in the vicinity of the Kerguelen Isles, found a velocity of 5.25 km s^{-1} on the profile EL47-25 (Fig. 2). The increase in velocity with depth is taken to correspond to the gradual closing of cracks and pores (Bunch & Kennett 1980).

High Poisson's ratios in the lower crust are consistent with an oceanic origin of the Kerguelen Isles and suggests likely high heat flow values regarding the age of the lithosphere and the crustal thickness.

As quoted above, the Poisson's ratio-depth behaviour (Fig. 9) resembles that calculated for oceanic regions (Spudich & Orcutt 1980) and supports the oceanic origin of the Kerguelen Isles.

On the other hand, this refraction work carried out in the Kerguelen Isles substantiates the oceanic origin of Broken Ridge. The Kerguelen–Gausberg Ridge and Broken Ridge were joined before anomaly 18 time and have almost the same velocity–depth behaviour. Francis & Raitt (1967) pointed out that the solid crustal thickness is down to 18 km, and concluded a 'quasi-continental' origin for Broken Ridge. Later, MacKenzie, Orcutt & McClain (1980),

computing synthetic seismograms, reinterpreted Francis & Raitt's data. The crustal thickness down to 18 km has been confirmed, but the velocity–depth behaviour resembles those observed in thick oceanic crust, i.e. aseismic ridges. These results are strengthened by the fact that Broken Ridge is edged, north, south and east by oceanic crust.

Veevers & Cotterill (1978) noticed that Broken Ridge and the Naturaliste Plateau are both north-dipping tilted blocks, truncated by a steep scarp on the south but not on the north. If these features were continental, they should be cut by marginal transform faults on the north because, as shown by magnetic anomalies, the spreading direction prior to the separation of Australia/Antarctica was at right angles to the trend of most of the northern flank. Moreover, a northern extension of Broken Ridge lies on undisputed oceanic crust that post-dates the inception of spreading (Markl 1974). These observations are in accord with the hypothesis for the oceanic origin of the Kerguelen–Heard Ridge and that Kerguelen and Broken Ridge were joined together.

Like other islands, the origin of the Kerguelen Isles is ascribed to the displacement of the Antarctica plate over a hot spot (Luyendyk & Rennick 1977; Duncan 1981). However, data from Goslin, Recq & Schlich (1981b) showed that these displacements are not linear; the results of Giret (1983) and Wicquart (1983) are not consistent with the hot spot hypotheses, while Houtz *et al.* (1977), Goslin *et al.* (1981b) and Mutter & Cande (1983) have shown that the western part of the Kerguelen–Gaussberg Ridge was originated by a ridge jump. Reconstruction to total closure causes an unacceptable overlap of Broken Ridge and Kerguelen–Gaussberg Ridge. This has been partially resolved inthe past by supposing that the northern part of Kerguelen–Gaussberg Ridge, principally involved in the overlap, is younger than the remainder. Mutter & Cande (1983) revised the early reconstructions using a newly proposed break up chronology of Australia and Antarctica which suggests that opening starts at least 90 Ma at an initially low rate. This eliminates the overlap and is consistent with the age of the Kerguelen–Gaussberg Ridge. The north-eastern flank of the ridge may be underlain by the 'missing' westward continuation of the Diamantina fracture zone. It may have isolated on the Antarctica plate by a ridge crest jump at anomaly 24 time.

Conclusion

Geological and geochemical investigations in the Kerguelen Isles show the previously suggested continental structure of the Kerguelen archipelago and the Kerguelen–Gaussberg Ridge to be doubtful. The first refraction experiment conducted in an oceanic island of the southern Indian Ocean shows in Kerguelen a velocity–depth behaviour similar to that found in thick oceanic features generated near active spreading ridges, i.e. the Crozet Rise and the Madagascar Ridge. Excessive volcanism along segments of the East Indian Ridge supports the oceanic origin of the Kerguelen–Gaussberg Ridge. The mean crustal thickness ranges from 14 to 16 km, even less in Val Studer. Seismic data invalidate earlier hypotheses for the existence of a 23 km deep crustal root beneath the Kerguelen–Heard Ridge. Near isostatic compensation is achieved by a low density mantle beneath the ridge. This scheme implies an upwelling of partially melted mantle. The magnetic anomaly pattern demonstrates that the Kerguelen–Gaussberg Ridge and Broken Ridge were joined prior to anomaly 18 time (40–42 Ma); hence, the oceanic structure of Kerguelen implies a same origin for Broken Ridge.

This preliminary work has to be supplemented by more extended profiles across the entire archipelago to investigate the central and western part of the archipelago, and some features such as the Mont Ross and the ring complex of the Rallier du Baty Peninsula.

Acknowledgments

This work would not have been possible without the efforts at sea and on land of Daniel Brefort (IPGP), Jacques Brechet, Jacques Bulle, Alain Lamaille (TAAF), Denis Malan (Nitro Bickford), the crew of *N/O La Japonaise*, Capitaine Jean-François Germain and his colleagues of the French Armée de l'Air. This programme would not have reached completion without the advice and assistance of Bernard Morlet and Jacques Duboys de la Vigerie from Terres Australes et Antarctiques Françaises (TAAF), Alfred Hirn and Jean-Louis Veinante from Institut de Physique du Globe de Paris, and Jacques Nougier from the Université d'Avignon. This article has been partly written at the Bullard Laboratories, University of Cambridge, and we are grateful to Dr Carol Williams for comments and improvements to the text, and also to Dr George Spence and Dr Martin Sinha who provided us with computer time and assistance in order to perform synthetic seismograms. We would like to thank Robert Headland of the Scott Polar Research Institute for bibliographical investigations on early scientific voyages in the southern Indian Ocean.

Financial support for the experiment came from Terres Australes et Antarctiques Françaises, the Groupe d'Etude de la Marge Continentale (UA 718 of CNRS), the Laboratoire d'Etude Géophysique des Structures Profondes (LA195 du CNRS) and the ATP 'Transfers' of the Institut National des Sciences de l'Univers. Contribution GEMC no. 329. Contribution IPGP no. 841.

References

Arons, A., Slifko, J. & Carter, A., 1948. Secondary pressure pulses due to gas globe oscillation in underwater explosions, *J. acoust. Soc. Am.*, **20**, 3.

Aubert de la Rüe, E., 1932. Etude géologique et géographique de l'archipel de Kerguelen, *Rev. Géogr. phys. Géol. dyn.*, **5**, 231 pp.

Ballestracci, R., Nougier, J. & Benderitter, Y., 1983. Mise en évidence et interprétation d'une zone électriquement conductrice dans les basaltes des plateaux des îles Kerguelen (TAAF), *C. r. Acad. Sci., Paris*, II, **296**, 833–838.

Barrett, D. M., 1977. Agulhas Plateau off Southern Africa: a geophysical study, *Bull. geol. Soc. Am.*, **88**, 749–763.

Bauer, A. & Berthois, L., 1963. Activité volcanique dans l'île Kerguelen, *Com. natl. Fr. Rech. Antarct.*, **2**, 79–105.

Bowin, C. O., 1973. Origin of the Ninetyeast Ridge from studies near the Equator, *J. geophys. Res.*, **78**, 6029–6043.

Bunch, A. W. H. & Kennett, B. L. N., 1980. The crustal structure of the Reykjanes Ridge, *Geophys. J. R. astr. Soc.*, **61**, 141–166.

Case, J. E., Ryland, S. L., Simkin, T. & Howard, K. A., 1973. Gravitational evidence for a low-density mass beneath the Galapagos Islands, *Science*, **181**, 1040–1042.

Chapman, C. H. & Drummond, R., 1982. Body-wave seismograms in inhomogeneous media using Maslov asymptotic theory, *Bull. seism. Soc. Am.*, **6**, S277–S317.

Charvis, P., 1984. Etude de la structure profonde de deux rides asismiques de l'Océan Indien: les plateaux sous-marins de Kerguelen-Heard et de Crozet, unpublished, *Thèse de 3ème cycle*, Université Pierre et Marie Curie.

Christensen, N. I. & Salisbury, M. H., 1975. Structure and constitution of the lower oceanic crust, *Rev. Geophys. Space Phys.*, **13**, 57–86.

Chun, C., 1900. *Aus den Tiefen des Weltmeeres*, Gustav Fischer, Iena.

Dietz, R. S. & Holden, J. C., 1970. Reconstruction of Pangea: breakup and dispersion of continents, Permian to present, *J. geophys. Res.*, **75**, 4939–4950.

Dobrin, M. D., 1976. *Introduction to Geophysical Prospecting*, 3rd edn. McGraw-Hill, New York.

Dosso, L. & Murthy, V. R., 1980. A Nd isotopic study of Kerguelen islands: inferences on enriched oceanic mantle sources, *Earth planet. Sci. Lett.*, **48**, 268–276.

Dosso, L., Vidal, P., Cantagrel, J. M., Lameyre, J., Marot, A. & Zimine, S., 1979. Kerguelen, continental

fragment or oceanic island? Petrology and isotopic geochemistry evidence, *Earth planet. Sci. Lett.*, **43**, 46–60.

Duncan, R. A., 1981. Hot spots in the southern oceans, an absolute frame of reference for motion of Gondwana continents, *Tectonophys.*, **74**, 29–42.

Dupré, B. & Allègre, C. J., 1983. Pb-Sr isotope variation in Indian Ocean basalts and mixing phenomena, *Nature*, **303**, 142–146.

Duschenes, J., 1983. Aspects of ocean bottom seismology, unpublished *PhD thesis*, University of Cambridge.

Ewing, M., Houtz, R. & Hayes, D. E., 1972. The Kerguelen Plateau (abstract), *Proc. Int. Geol. Congr. 24th*, Montréal, p. 257.

Fowler, C. M. R., 1976. Crustal structure of the Mid-Atlantic Ridge crest at 37°, *Geophys. J. R. astr. Soc.*, **47**, 459–491.

Fowler, C. M. R., 1978. The Mid-Atlantic Ridge: structure at 45°N, *Geophys. J. R. astr. Soc.*, **54**, 167–184.

Francis, T. J. G. & Raitt, R. W., 1967. Seismic refraction measurements in the southern Indian Ocean, *J. geophys. Res.*, **72**, 3015–3041.

Francis, T. J. G. & Shor, G. G., 1966. Seismic refraction measurements in the northwest Indian Ocean, *J. geophys. Res.*, **71**, 427–449.

Fröhlich, F. and the scientific party of MD 35 cruise, 1983. Mise en évidence d'une série sédimentaire pélagique du Paléocène et du Crétacé supérieur sur le plateau de Kerguelen: résultats préliminaires de la campagne océanographique MD35/D.R.A.K.A.R., *C. r. Acad. Sci., Paris*, **297**, 153–156.

Gérard, A., Lesquer, A., Lachaud, J. C., Louis, P. & Mennechet, C., 1980. Etude gravimétrique de la moitié sud-est de l'île de la Réunion, *C. r. Acad. Sci., Paris, B*, **290**, 139–142.

Giret, A., 1980. Carte géologique au 1/50.000 de la péninsule Rallier du Baty, *Com. natl. Fr. Rech. Antarct.*, **45**.

Giret, A., 1983. Le plutonisme océanique intraplaque. Exemple de l'archipel Kerguelen. Terres Australes et Antarctiques Françaises, *Thesis*, Université Pierre et Marie Curie, Paris.

Goslin, J., 1981. Etude géophysique des reliefs asismiques de l'Océan Indien occidental et austral, *Thesis*, Université Louis Pasteur, Strasbourg.

Goslin, J. & Patriat, P., 1984. Absolute and relative plate motions and hypotheses on the origin of five aseismic ridges in the Indian Ocean, *Tectonophys.*, **101**, 221–244.

Goslin, J., Recq, M. & Schlich, R., 1981a. Structure profonde du plateau de Madagascar: relations avec le plateau de Crozet, *Tectonophys.*, **76**, 75–97.

Goslin, J., Recq, M. & Schlich, R., 1981b. Mise en place et évolution des plateaux sous-marins de Madagascar et de Crozet, *Bull. Soc. géol. Fr.*, **6**, 609–618.

Hales, A. L. & Nation, J. B., 1973. A seismic refraction study in the southern Indian Ocean, *Bull. seism. Soc. Am.*, **63**, 1951–1966.

Heezen, B. C. & Tharp, M., 1965. Tectonic fabric of the Atlantic and Indian Oceans and continental drift, *Phil. Trans. R. Soc. A*, **258**, 90–106.

Hill, D. P., 1969. Crustal structure of the island of Hawaii from seismic-refraction measurements, *Bull. seism. Soc. Am.*, **59**, 101–130.

Houtz, R. E., Hayes, D. E. & Markl, R. G., 1977. Kerguelen Plateau bathymetry sediment distribution and crustal structure, *Mar. Geol.*, **25**, 95–130.

Johnson, G. L. & Palmason, G., 1980. Observations of the morphology and structure of the sea floor West of Iceland, *J. Geophys.*, **1–3**, 23–30.

Kinoshita, W. T., Krivoy, H. L., Mabey, D. R. & McDonald, R. R., 1963. Gravity survey of the island of Hawaii. *Prof. Pap., U.S. geol. Surv., 475-C*, 114–116.

Lameyre, J., Marot, A., Zimine, S., Cantagrel, J. M., Dosso, L. & Vidal, P., 1976. Chronological evolution of the Kerguelen island syenite-granite ring complex, *Nature*, **265**, 306–307.

Lameyre, J., Marot, A., Zimine, S., Cantagrel, J. M., Dosso, L., Vidal, P., Giret, A., Joron, J. L., Treuil, M. & Hottin, G., 1981. Etude géologique du complexe plutonique de la péninsule Rallier du Baty, îles Kerguelen, *Com. natl. Fr. Rech. Antarct.*, **49**, 175p.

Le Pichon, X. & Heirtzler, J., 1968. Magnetic anomalies in the Indian Ocean and sea-floor spreading, *J. geophys. Res.*, **73**, 2101–2117.

Ludwig, W. J., Nafe, J. E. & Drake, C. L., 1970. Seismic refraction, in *The Sea*, 4, part 1, pp. 53–64, ed. Maxwell, A. E., Wiley, New York.

Ludwig, W. J., Nafe, J. E., Simpson, E. S. W. & Sacks, S., 1968. Seismic refraction measurements on the southeast African continental margin, *J. geophys. Res.*, **73**, 3707–3719.

Luyendyk, B. P. & Rennick, W., 1977. Tectonic history of aseismic ridges in the eastern Indian Ocean, *Bull. geol. Soc. Am.*, **88**, 1347–1356.

MacKenzie, K. R., Orcutt, J. A. & McClain, J. S., 1980. Crustal structure of the Broken Ridge, *EOS*, **46**, 1049.

McKenzie, D. P. & Sclater, J. G., 1971. The evolution of the Indian Ocean since Late Cretaceous, *Geophys. J. R. astr. Soc.*, **25**, 457–528.

McKenzie, D. P. & O'Nions, R. K., 1983. Mantle reservoirs and ocean islands basalts, *Nature*, **301**, 229–231.

Markl, R. G., 1974. Evidence for the break up of eastern Gondwanaland by the Early Cretaceous, *Nature*, **251**, 196–199.

Marot, A. & Zimine, S., 1976. Les complexes annulaires de syénites et granites alcalins dans la péninsule Rallier du Baty, îles Kerguelen (TAAF), *Thèse de 3è cycle*, Université Pierre et Marie Curie, Paris.

Matthews, D. H. & Davies, D., 1966. Geophysical studies of the Seychelles Bank, *Phil. Trans. R. Soc.*, **259**, 227–239.

Michel, B. & Hirn, A., 1980. Velocity–depth estimation from wide angle seismic reflection arrivals, *Annls Géophys.*, **36**, 107–118.

Murray, J. & Renard, A. F., 1885. *Report of scientific results of the exploring voyage of H. M. S. Challenger (1873–1876). Deep-sea deposits*, Longmans and Co, London.

Mutter, J. C. & Cande, S. C., 1983. The early opening between Broken Ridge and Kerguelen Plateau, *Earth planet. Sci. Lett.*, **65**, 369–376.

Norton, I. O. & Molnar, P., 1977. Implications of revised fit between Australia and Antarctica for the evolution of the eastern Indian Ocean, *Nature*, **267**, 330–340.

Nougier, J., 1970. Contribution à l'étude géologique et géomorphologique des îles Kerguelen (Terres Australes et Antarctiques Françaises), *Com. natl. Fr. Rech. Antarct.*, **27**, 246p.

Nougier, J., 1972. Geochronology of the volcanic activity in Iles Kerguelen, in *Antarctic Geology and Geophysics*, pp. 803–808, ed. Adie, R. J., Universitetsforlaget, Oslo.

Nougier, J., Ballestracci, R. & Blavoux, B., 1982. Les manifestations postvolcaniques dans les îles australes (TAAF). Zones fumerolliennes et sources thermo-minérales, *C. r. Acad. Sci., Paris*, **295**, 389–392.

Nougier, J. & Lameyre, J., 1973. Les nordmarkites des îles Kerguelen (TAAF) dans leur cadre structural. Problème de leur origine et de celle de certaines roches plutoniques alcalines en domaine océanique, *Bull. Soc. Géol. Fr.*, **7**, 306–311.

O'Brien, P. N. S., 1960. Seismic energy from explosions, *Geophys. J. R. astr. Soc.*, **3**, 29–44.

Orcutt, J. A., Kennett, B. L. N. & Dorman, L. M., 1976. Structure of the East Pacific Rise from an ocean bottom seismometer survey, *Geophys. J. R. astr. Soc.*, **45**, 305–320.

Palmason, G., 1970. *Crustal Structure of Iceland from Explosion Seismology*, Science Institute, University of Iceland and National Energy Authority, Reykjavik.

Patriat, P., 1983. Evolution de l'Océan Indien depuis le Crétacé supérieur, *Thèse de Doctorat d'Etat*, Université Pierre et Marie Curie, Paris.

Philippi, E., 1912. Geologische Beobachtungen auf Kerguelen, pp. 187–207, and Geologie der Heard Insel, pp. 243–250, in *Deutsche Süd-Polar Expedition* (see Von Drygalski 1912).

Purdy, G. M., 1983. The seismic structure of 140 Myr old crust in the western central Atlantic Ocean, *Geophys. J. R. astr. Soc.*, **72**, 115–137.

Recq, M., 1983. Anomalies isostatiques sous le bassin de Crozet et la dorsale est-indienne, *Bull. Soc. géol. Fr.*, pp. 53–62.

Recq, M. & Charvis, P., 1985. Deep seismic soundings in the Kerguelen Isles. EUG III Meeting, Strasbourg, April 1985, *Terra Cognita*, **2–3**, p. 176.

Recq, M., Charvis, P. & Hirn, A., 1983. Premières données sur la structure profonde de la ride de Kerguelen, d'après les résultats de réfraction sismique, *C. r. Acad. Sci., Paris*, **297**, 903–908.

Recq, M. & Goslin, J., 1981. Etude de l'équilibre isostatique dans le Sud-Ouest de l'Océan Indien à l'aide des résultats de réfraction sismique, *Mar. Geol.*, pp. M1–M10.

Recq, M., Goslin, J., Patriat, P. & Schlich, R., 1979. Profils de réfraction sur le plateau malgache, Résultats préliminaires, *7ème Réun. Ann. Sci. Terre*, p. 394, Lyons, Societé géologiques de France.

Roth, J., 1875. Ueber Gesteine von Kerguelensland, *Mber. K. Preuss. Akad. wiss.*, November.

Rouillon, G., 1963. Bouguer gravity anomaly map of Kerguelen Islands, *Terres australes antarct. fr.*, unpublished data.

Ryall, A. & Bennett, D. E., 1968. Crustal structure of southern Hawaii related to volcanic processes in the upper mantle, *J. geophys Res.*, **73**, 4561–4582.

Schlich, R., 1975. Structure et âge de l'Océan Indien occidental, *Mém. hors–série, Soc. géol. Fr.*, **6**, 102 pp.

Schlich, R., 1983. The Indian Ocean: aseismic ridges, spreading centres, and ocean basins, in *The Ocean Basins and Margins, vol. 6: The Indian Ocean,* eds Nairn, A. E. M. & Stehli, F. G.

Schlich, R. & Patriat, P., 1971. Anomalies magnétiques de la branche Est de la médio-indienne entre les îles Amsterdam et Kerguelen, *C. r. Acad. Sci., Paris,* **272,** 773–776.

Schlich, R., Delteil, J. R., Moulin, J., Patriat, P. & Guillaume, R., 1971. Mise en évidence d'une sédimentation de marge continentale sur le plateau de Kerguelen-Heard, *C. r. Acad. Sci., Paris,* **272,** 2060–2065.

Sinha, M. C. & Louden, K. E., 1983. The Oceanographer fracture zone – I. Crustal structure from seismic refraction studies, *Geophys. J. R. astr. Soc.,* **75,** 713–736.

Sinha, M. C., Louden, K. E. & Parsons, B., 1981. The crustal structure of the Madagascar Ridge, *Geophys. J. R. astr. Soc.,* **66,** 351–377.

Spudich, P. & Orcutt, J., 1980. Petrology and porosity of an oceanic crustal site: results from wave form modeling of seismic refraction data, *J. geophys. Res.,* **85,** 1409–1433.

Stephen, R. A., 1978. The oblique seismic experiment in oceanic crust, *PhD thesis,* University of Cambridge.

Stephenson, P., 1964. Some geological observations on Heard Islands, *Antarctic Geology,* pp. 14–24, ed. Adie, R. J., North Holland, Amsterdam.

Studer, J., 1878. Geologische Beobachtungen auf Kerguelensland, *Z. dt. geol. Ges.,* **2,** 327–350.

Studer, J., 1889. *Forschungreise SMS 'Gazelle', 1874–1876,* vol. II, Mittler & Sohn, Berlin.

Talwani, M., Windisch, C. C. & Langseth (Jr), M. G., 1971. Reykjanes Ridge: a detailed geophysical study, *J. geophys. Res.,* **76,** 473–517.

Vanney, J. R. & Johnson, G. L., 1982. Marine geomorphology of Kerguelen–Antartica Passage (southern Indian Ocean), in *The Sea Floor,* pp. 237–254, eds Scrutton, R. A. & Talwani, M., Wiley, London.

Veevers, J. J. & Cotterill, D., 1978. Western margin of Australia: evolution of a rifted arch system, *Bull. geol. Soc. Am.,* **89,** 337–355.

Von Drygalski, E., 1912. *Deutsche Süd-Polar Expedition,* vol. II, Georg Reimer, Berlin.

Watkins, N. D., Gunn, B. M., Nougier, J. & Baski, A. K., 1974. Kerguelen: continental fragment or oceanic island? *Bull. geol. Soc. Am.,* **85,** 201–212.

Watts, A. B. & Cochran, J. R., 1974. Gravity anomalies and flexure of the lithosphere along the Hawaiian-Emperor seamount chain, *Geophys. J. R. astr. Soc.,* **38,** 119–141.

White, R. S., 1979. Oceanic upper crustal structure from variable angle seismic reflection-refraction profiles, *Geophys. J. R. astr. Soc.,* **57,** 683–726.

White, R. S. & Bunch, A. W. H., 1978. Explosive sink rates, *Geophys. J. R. astr. Soc.,* **56,** 473–476.

White, R. S. & Purdy, G. M., 1983. Crustal velocity structure on the flanks of Mid-Atlantic Ridge at 24° N, *Geophys. J. R. astr. Soc.,* **75,** 361–385.

Wicquart, E., 1983. Modèle lithostratigraphique du plateau de Kerguelen-Heard (Océan Indien), *Thèse de 3ème cycle,* Université Pierre et Marie Curie, Paris.

Wilson, J. T., 1965. Evidence from ocean islands suggesting movements in the Earth, *Phil. Trans. R. Soc. A,* **258,** 145–167.

Zhivago, A. V., 1965. Géomorphologie et tectonique du fond de l'Océan Antarctique, *Rech. Océan.,* **13,** Sci. Moscow, trans. *Com. natl. Fr. Rech. Antarct.,* **17,** 19–26.

Zucca, J. J. & Hill, D. P., 1980. Crustal structure of the southeast flank of Kilauea volcano, Hawaii, from seismic refraction measurements, *Bull. seism. Soc. Am.,* **70,** 1149–1159.

Zucca, J. J., Hill, D. P. & Kouach, R. L., 1982. Crustal structure of Mauna Loa volcano, Hawaii, from seismic refraction and gravity data, *Bull. seism. Soc. Am.,* **72,** 1535–1550.